

UNCLASSIFIED

AD NUMBER: AD0083341

LIMITATION CHANGES

TO:

Approved for public release; distribution is unlimited.

FROM:

Distribution authorized to U.S. Gov't. agencies and their contractors; Administrative/Operational Use; 1 Feb 1956. Other requests shall be referred to Office of Naval Research, Washington, DC.

AUTHORITY

ONR LTR 9 NOV 1977

**THIS REPORT HAS BEEN DELIMITED  
AND CLEARED FOR PUBLIC RELEASE  
UNDER DOD DIRECTIVE 5200.20 AND  
NO RESTRICTIONS ARE IMPOSED UPON  
ITS USE AND DISCLOSURE.**

**DISTRIBUTION STATEMENT A**

**APPROVED FOR PUBLIC RELEASE;  
DISTRIBUTION UNLIMITED.**

---

**AD**

**83341**

# Armed Services Technical Information Agency

Reproduced by  
**DOCUMENT SERVICE CENTER**  
**KNOTT BUILDING, DAYTON, 2, OHIO**

This document is the property of the United States Government. It is furnished for the duration of the contract and shall be returned when no longer required, or upon recall by ASTIA to the following address:  
Armed Services Technical Information Agency, Document Service Center,  
Knott Building, Dayton 2, Ohio.

**NOTICE: WHEN GOVERNMENT OR OTHER DRAWINGS, SPECIFICATIONS OR OTHER DATA ARE USED FOR ANY PURPOSE OTHER THAN IN CONNECTION WITH A DEFINITELY RELATED GOVERNMENT PROCUREMENT OPERATION, THE U. S. GOVERNMENT THEREBY INCURS NO RESPONSIBILITY, NOR ANY OBLIGATION WHATSOEVER; AND THE FACT THAT THE GOVERNMENT MAY HAVE FORMULATED, FURNISHED, OR IN ANY WAY SUPPLIED THE SAID DRAWINGS, SPECIFICATIONS, OR OTHER DATA IS NOT TO BE REGARDED BY IMPLICATION OR OTHERWISE AS IN ANY MANNER LICENSING THE HOLDER OR ANY OTHER PERSON OR CORPORATION, OR CONVEYING ANY RIGHTS OR PERMISSION TO MANUFACTURE, USE OR SELL ANY PATENTED INVENTION THAT MAY IN ANY WAY BE RELATED THERETO.**

**UNCLASSIFIED**

AD No. 83341

ASTIA FILE COPY

REPORT NO. 49

DECOMPOSITION OF  
HYDROGEN PEROXIDE VAPOR

FC

Prepared for the  
Office of Naval Research  
Contract No. N5ori-07819  
NR-092-008

Reproduction in whole or in part is permitted for any purpose  
by the United States Government

83341

BY

C. N. Satterfield  
T. W. Stein

MASSACHUSETTS INSTITUTE OF TECHNOLOGY  
Department of Chemical Engineering Cambridge, Mass.

Division of Industrial Cooperation Project 6552  
February 1, 1956

REPORT NO. 49

**DECOMPOSITION OF  
HYDROGEN PEROXIDE VAPOR**

Prepared for the  
Office of Naval Research  
Contract No. N5ori-07819  
NR-092-008

Reproduction in whole or in part is permitted for any purpose  
by the United States Government

BY

C. N. Satterfield  
T. W. Stein

**MASSACHUSETTS INSTITUTE OF TECHNOLOGY**  
Department of Chemical Engineering      Cambridge, Mass.

Division of Industrial Cooperation Project 6552  
February 1, 1956

## INTRODUCTION

The heterogeneous decomposition of hydrogen peroxide vapor has been the subject of several investigations. Data have been reported for the rates of decomposition at partial pressures of hydrogen peroxide from 5 or 6 mm of mercury up to 1 or 2 cm, at temperatures from room temperature up to 400°C, and on such surfaces as soft glass, Pyrex, quartz, aluminum and tin. The work of previous investigators has been recently summarized (30). However, there have been many inconsistencies in the data available and an explanation of the fundamental nature of the heterogeneous decomposition of hydrogen peroxide vapor has been lacking. One of the purposes of this work was to try to obtain a clearer picture of the important factors which affect the surface decomposition rate. A second objective was to ascertain under what conditions homogeneous decomposition becomes appreciable. Aside from these more theoretical reasons, there is an engineering need for determining those materials which will cause the minimum decomposition on contact with hydrogen peroxide vapor. In the present work substantially greater H<sub>2</sub>O<sub>2</sub> vapor concentrations than previously were studied, as well as a much greater variety of surfaces.

Previous studies indicate that any surface has an accelerating effect on hydrogen peroxide vapor decomposition. Most investigators have reported that the reaction rate can be expressed by a first order equation, although second order reactions, both retarded and unretarded by water, and zero reactions have also been suggested (10,16,17). The reaction is reportedly unretarded by additions of moderate quantities of air, or CO<sub>2</sub>.

The rate of reaction is much higher on metals or soft glass than on Pyrex or quartz although it can be varied by one or more orders of magnitude on a Pyrex surface alone by changing its chemical and physical properties. The reported activation energies have ranged from 5-20 Kcal./gm.mole, but most frequently have been in the vicinity of 10 Kcal./gm.mole.

The homogeneous decomposition of hydrogen peroxide vapor has been observed primarily only in studies of flames and explosions. The explosion limits of hydrogen peroxide vapor at various total pressures have been determined (28,29) and it was found that these limits were dependent only on the hydrogen peroxide concentration in the vapor and were unaffected by the ratio of water to oxygen. The decomposition of the vapor in boric oxide reaction tubes in the temperature range from 470-540°C has been observed (19) and an activation energy was reported that was in the range of 40-50 Kcal./gm.mole. On the basis of the magnitude of this quantity and the effect observed when the surface to volume ratio of the reaction tubes were changed, it was concluded that the decomposition was at least partially homogeneous.

## EXPERIMENTAL

The experimental apparatus comprised two sections, a vaporization section, depicted on Figure 1, and a decomposition section, shown in Figure 2.

The vaporization section was capable of producing a steady flow of hydrogen peroxide vapor at a constant concentration. A hydrogen peroxide-water solution was fed continuously to an electrically-heated Pyrex boiler through a levelling device (see insert on Figure 1) which maintained a constant liquid level in the boiler. The boiler pressure was regulated by an external helium system; the helium, being lighter than the hydrogen peroxide-water vapors, was prevented from entering the system by maintaining in the reflux condenser, atop the boiler, a helium-vapor interface, which is visible.

The hydrogen peroxide-water vapor mixture from the boiler first passed through an entrainment separator and then through an electrically heated Pyrex preheater (see Figure 2). A portion of the vapor at this point was withdrawn for analysis by condensing it at 5°C, and analysing the condensate for hydrogen peroxide content by potassium permanganate titration. The remainder of the vapor flowed through the reaction tube, and was then similarly condensed and analysed. The division of vapor flow between the upstream and downstream condensers was controlled by control of the pressure, this being set by bubbling the oxygen leaving each condenser through a column of water before passing it through a wet test meter. The collectors in which the liquid samples accumulated were so constructed that the samples could be removed without affecting the pressures in the condensers, so as not to affect the flow division.

The reaction tubes used in the study of glass surfaces were usually one inch in diameter and approximately two foot long, with ball and socket joints on the ends with which the tube was clamped in the system. When plastic surfaces were to be studied, the samples were placed in the glass reaction tubes. In the study of metallic surfaces, metal rods about 3/32 inches in diameter and 6.5 inches long rested coaxially, on small aluminum supports, in a Pyrex tube about one foot long. The ends of this Pyrex tube had a diameter of one inch, but the central portion in which the metallic sample was placed had a diameter of 3/16 inches.

Each reaction tube was immersed in a constant temperature bath to which it was sealed by stuffing boxes, using asbestos tape as the gasketing material. At temperatures below 180°C, "Nujol", a mineral oil, was used in the bath; at temperatures above 180°C, a molten salt mixture containing 7 wt.% sodium nitrate, 40 wt.% sodium nitrite, and 53 wt.% potassium nitrate, was used. The bath was agitated by a stirrer and its temperature was regulated to within  $\pm 2^\circ\text{C}$  by a thermostat which controlled a heater lying along the length of the bath. The temperatures were measured with iron-constantan thermocouples at three locations--in a well at the exit of the preheater and in the two ends of the constant temperature bath.

The range of experimental variables studied in this work was:

Partial pressure of hydrogen peroxide	0.02-0.23 atm.
Temperature	110-490°C
Total pressure	1 atm.

The partial pressures of hydrogen peroxide studied were higher than those hitherto investigated and closer to those likely to be encountered in practical operations.

The data obtained in each set of experimental conditions were the amount and composition of the hydrogen peroxide-water liquid sample collected from each condenser, the volume of oxygen leaving each condenser, the upstream and downstream pressures, the temperature of the vapor leaving the preheater and the temperature of the bath. At each of the combinations of experimental conditions, three sets of data were collected to avoid fortuitous errors. By means of a material balance, the rate at which each component enters and leaves the reaction tube can be calculated and from this the rate of decomposition of the hydrogen peroxide.

Except for a few runs at the very highest temperatures studied, the inlet and exit concentrations were not greatly different, so that the reaction tube may in general be regarded as a "differential reactor". The correct method of averaging inlet and exit concentrations is therefore relatively unaffected by the order of the reaction. If, for example, the inlet and outlet partial pressures were to differ by as much as a factor of 2, the log-mean partial pressure, the correct mean for a first order reaction, would differ from the geometric-mean, the correct mean for a second order reaction, by only 1.5%. The differential rate of decomposition, 
$$\frac{-dN_{H_2O_2}}{A \, dO}$$

is therefore calculated as the difference between the rate at which hydrogen peroxide enters and leaves the tube, divided by the total surface area. A few surfaces, Pyrex coated with boric oxide and 2S aluminum, were studied over a range of temperatures and compositions sufficiently extensive that the results could be expressed in a mathematical form based on the Langmuir adsorption model. Other surfaces were studied less extensively and frequently at only one temperature. In these cases the activity of a surface is expressed by plotting the differential rate of decomposition observed against the geometric mean of the inlet and exit partial pressure of hydrogen peroxide. The partial pressure of oxygen and water vapor might also have some slight effect, but essentially the same concentration of liquid hydrogen peroxide was boiled in all studies of surface activities so that the concentrations of oxygen and water vapor were functions of the average hydrogen peroxide concentration only. The independent variables were thus reduced to three--the type of surface, temperature, and the partial pressure of hydrogen peroxide.

The rates of heterogeneous reaction studied here were sufficiently low that the rate of diffusion of  $H_2O_2$  from the bulk vapor to the surface was neglected as a limiting factor. This introduces a slight error in a few cases. Thus, the difference between the interfacial and bulk partial pressure was estimated, by means of the correlation for laminar flow in a wetted wall column (32), to be about 15% in the studies with the most reactive glass tube (tube 17,

a Pyrex tube with silver present) when the average bulk partial pressure of hydrogen peroxide was 0.02 atm. In an average Pyrex tube (tube 19) the maximum error was only 8% at an averaged bulk partial pressure of about .04 atm. This diffusional error would not affect the qualitative comparison of two surfaces because the error is greater on the more reactive surface. For those surfaces on which a wide range of hydrogen peroxide concentrations were studied and for which equations were derived, the difference is greater at the higher concentrations than at the lower. For example, on a boric oxide coated tube (tube 9) at 180°C the difference increased from 2% at 0.03 atmosphere of hydrogen peroxide partial pressure to 11% at a partial pressure of 0.2 atm. Similarly on an aluminum surface it increased from 3% at a bulk hydrogen peroxide partial pressure of 0.045 atm. to 13% at 0.14 atm. However neglecting the effect does not affect the form of the equation derived for expressing the data, and the value of the correction factor called for is generally less than the reproducibility of the data.

In studies of heterogeneous decomposition where a reaction tube itself was the surface studied, the area on which the reported rate is based was taken to be the entire area of the tube, including the slight portion which protruded outside the bath. The connectors to upstream and downstream condensers were acid-treated Pyrex and had an area of about 5% of the reaction tube. Except when studying the most inert surfaces, any decomposition on connector surfaces could be neglected; in a few cases a small correction factor was applied based on the known decomposition rate on acid-treated Pyrex.

## RESULTS AND DISCUSSION

The experimental results are given in Table I.

### Heterogeneous Decomposition

#### 1. Glass

Glass surfaces of various compositions were studied most extensively because they are the least active surfaces known. Various alterations were made in the chemical and physical natures of the glass surfaces in order to find what factors affect the decomposition rate of the vapor. Attempts were then directed towards removing or avoiding those elements which are the sources of catalytic activity on a surface.

#### Unaltered Surfaces

The rates of decomposition of hydrogen peroxide vapor were measured on the following commercially available glass surfaces, in the form of glass tubes: fused silica, boric oxide fused onto Pyrex, soft glass and lead glass. Several of the tubes were subjected to various chemical treatments to alter their surface. To distinguish between the subsequent differences in behaviour, the tube condition after each of these treatments is designated by a different letter.

Boric oxide films were fused onto several Pyrex tubes by a method suggested by Cook (4). The rates of hydrogen peroxide vapor decomposition on these surfaces are shown on Figure 3. Tube 7



REV	T <sub>AV</sub>	P <sub>1</sub>	P <sub>2</sub>	P <sub>3</sub>	P <sub>4</sub>	A	F
<b>STEP 7 (Condition A)</b>							
PIVOT							
99A	180	.029	.028	1.001	.009	.8227	1.61
B		.027	.026	1.000	.008	.1963	0.78
C		.032	.030	0.993	.010	.1479	0.94
99A	215	.040	.034	0.998	.009	.1741	1.09
B		.038	.027	0.994	.007	.2853	1.43
C		.027	.020	0.999	.007	.2437	1.52
99A	280	.030	.029	1.000	.008	.2443	2.62
B		.028	.027	1.000	.008	.2823	2.04
C		.026	.021	1.000	.008		
<b>STEP 7 (Condition B)</b>							
PIVOT WITH C-CLAMP AND BUSH							
99A	180	.033	.044	.974	.007	.0934	1.21
B		.024	.023	.964	.008	.0788	0.70
C		.025	.030	0.968	.008	.0437	0.48
99A	180	.033	.032	.999	.008	.1662	0.29
B		.030	.029	.994	.007	.1761	0.47
C		.034	.031	.999	.007	.1648	.81
99A	215	.045	.040	.980	.008	.1470	1.09
B		.030	.048	.974	.008	.1077	0.81
C							
99A	215	.039	.038	.987	.008	.2284	0.84
B		.038	.036	.984	.008	.2044	0.57
C							
99A	280	.024	.023	.999	.008	.1107	0.50
B		.030	.028	.995	.008	.0940	0.34
C							
99A	280	.038	.036	.988	.008	.2170	1.18
B		.039	.038	.988	.008	.2015	1.55
C							
<b>STEP 7 (Condition C)</b>							
PIVOT							
99A	180	.060	.052	.974	.019	.2195	2.88
B		.049	.056	.944	.020	.2192	2.78
C							
99A	215	.058	.065	.948	.033	.1431	0.87
B		.064	.064	.961	.018	.1128	4.04
C							
99A	280	.057	.047	.945	.009	.2415	3.88
B		.050	.044	.947	.011	.2011	2.17
C		.048	.054	.956	.010	.2151	2.24
<b>STEP 7 (Condition D)</b>							
PIVOT WITH 60° SHIM AT BUSH							
99A	180	.077	.060	.940	.008	.30807	17.2
B		.071	.062	.982	.008	.3410	18.0
C		.064	.062	.970	.007	.3652	14.9
99A	180	.030	.018	.998	.011	.2530	4.41
B		.020	.019	.994	.012	.2451	4.74
C		.030	.018	.998	.012	.2545	4.63
99A	215	.067	.022	.979	.011	.1710	12.84
B		.073	.021	.974	.011	.1803	15.30
C		.069	.021	.972	.013	.1586	12.84
99A	215	.083	.017	.991	.014	.1944	5.11
B		.038	.016	.995	.012	.2017	6.56
C		.032	.018	.995	.012	.2402	8.89
99A	280	.028	.012	.946	.013	.1258	9.38
B		.028	.013	.943	.013	.1368	8.70
C		.028	.014	.988	.013	.1378	9.42
99A	280	.038	.018	1.000	.005	.2857	7.75
B		.038	.020	1.000	.004	.3277	7.97
C		.038	.022	1.01	.002	.4797	7.94
<b>STEP 7 (Condition E)</b>							
PIVOT WITH 60° SHIM AT BUSH							
99A	180	.064	.050	.937	.014	.2892	3.89
B		.072	.058	.955	.015	.2750	6.31
C		.060	.054	.958	.015	.2327	3.87
99A	180	.028	.026	.978	.010	.2904	0.71
B		.025	.027	.974	.014	.3035	1.07
C		.033	.028	.949	.012	.3154	2.35
99A	215	.059	.044	.944	.015	.2329	5.27
B		.055	.044	.949	.023	.1945	2.37
C		.058	.045	.939	.020	.2065	4.88
99A	215	.030	.028	.947	.014	.2023	0.76
B		.029	.024	.974	.012	.2416	1.39
C		.029	.028	.974	.012	.2572	1.52
99A	280	.060	.042	.941	.019	.2263	6.70
B		.058	.043	.940	.021	.2265	5.28
C		.053	.041	.943	.015	.1923	4.89
99A	280	.037	.028	.970	.010	.2009	4.47
B		.033	.029	.966	.014	.2797	1.57
C		.038	.027	.962	.012	.2341	2.08
<b>STEP 8</b>							
PIVOT WITH 60° SHIM AT BUSH							
99A	180	.042	.048	.940	.012	.1840	3.75
B		.065	.051	.940	.008	.2428	5.58
C		.070	.050	.931	.015	.1210	3.77
99A	180	.019	.015	.977	.012	.2789	1.71
B		.019	.016	.981	.014	.2471	1.20
C		.019	.017	.974	.014	.2436	1.08
99A	215	.045	.047	.932	.017	.1812	5.29
B		.064	.046	.934	.017	.1839	5.31
C							

REV	T <sub>AV</sub>	P <sub>1</sub>	P <sub>2</sub>	P <sub>3</sub>	P <sub>4</sub>	A	F
<b>STEP 8 (Condition A)</b>							
(Continued)							
99A	215	.027	.028	.988	.014	.2617	1.28
B		.032	.030	.992	.019	.1884	0.78
C		.027	.026	.986	.014	.2897	1.04
99A	280	.058	.044	.937	.019	.2523	6.82
B		.055	.043	.938	.020	.3373	6.88
C		.055	.046	.938	.021	.3297	5.99
99A	280	.030	.027	.940	.015	.2421	1.20
B		.030	.028	.944	.011	.3380	2.38
C		.031	.027	.943	.023	.1493	1.32
<b>STEP 8 (Condition B)</b>							
PIVOT WITH 60° SHIM AT BUSH							
99A	180	.020	.028	.994	.008	.2874	1.72
B		.028	.024	.990	.009	.2876	1.63
C							
99A	280	.037	.029	.991	.009	.2264	2.97
B		.024	.029	.991	.009	.2284	2.50
C		.038	.028	.998	.010	.2481	2.40
99A	215	.024	.028	.992	.008	.2738	2.79
B		.031	.028	.993	.010	.2798	1.20
C		.030	.028	.995	.008	.2733	0.78
<b>STEP 8 (Condition C)</b>							
PIVOT WITH 60° SHIM AT BUSH							
99A	180	.099	.089	.977	.022	.1228	6.21
B		.084	.070	.982	.018	.1148	4.93
C		.102	.067	.964	.019	.1052	6.00
99A	180	.030	.028	.974	.012	.2253	1.37
B		.029	.028	.974	.012	.2264	1.40
C		.029	.028	.974	.014	.2228	1.58
99A	180	.064	.049	.944	.013	.2484	6.00
B		.066	.051	.944	.010	.2643	6.23
C		.075	.058	.937	.013	.2458	7.60
99A	215	.028	.019	.977	.014	.2343	2.28
B		.028	.018	.978	.014	.2180	4.74
C		.028	.019	.980	.012	.2272	2.63
99A	215	.070	.047	.942	.015	.2744	1.28
B		.068	.045	.946	.012	.2877	10.85
C		.068	.044	.944	.015	.2842	10.78
99A	215	.093	.068	.902	.021	.2992	3.62
B		.092	.066	.905	.019	.2991	9.52
C		.092	.066	.905	.021	.2867	9.92
99A	280	.074	.040	.919	.029	.1816	10.00
B		.074	.040	.921	.028	.1814	11.00
C		.078	.042	.911	.032	.1923	10.10
99A	280	.024	.014	.977	.014	.2247	2.82
B		.021	.013	.948	.014	.2215	3.04
C		.023	.014	.953	.012	.2427	3.73
99A	280	.065	.039	.948	.020	.1958	8.75
B		.061	.037	.946	.017	.1949	13.28
C		.070	.039	.936	.024	.1747	5.82
<b>STEP 8 (Condition D)</b>							
PIVOT WITH 60° SHIM AT BUSH							
99A	180	.061	.051	.970	.016	.1612	5.22
B		.064	.029	.967	.018	.1524	4.44
C		.061	.027	.972	.016	.1541	3.50
99A	180	.037	.020	1.008	.010	.2284	7.28
B		.037	.020	1.003	.010	.2293	3.31
C							
99A	180	.038	.040	.942	.014	.1850	6.71
B		.100	.048	.936	.017	.1947	6.62
C		.098	.041	.941	.017	.1696	6.08
99A	180	.020	.019	.948	.008	.4332	39.6
B		.014	.017	.956	.005	.4309	40.4
C		.022	.014	.940	.004	.4205	40.5
99A	180	.166	.062	.890	.014	.4115	37.4
B		.157	.059	.893	.029	.4329	28.0
C		.155	.062	.896	.032	.4331	28.5
99A	215	.034	.008	.999	.012	.2579	4.46
B		.032	.008	.999	.012	.2640	4.09
C		.031	.007	.999	.013	.2649	3.92
99A	215	.067	.033	.944	.018	.2541	7.88
B		.061	.033	.917	.017	.2793	7.02
C		.054	.030	.917	.014	.2807	7.00
99A	215	.094	.031	.934	.028	.2941	12.45
B		.090	.030	.941	.026	.2949	12.28
C		.093	.030	.930	.029	.3079	12.9
99A	215	.197	.081	.865	.041	.4685	41.2
B		.199	.065	.861	.042	.4529	39.8
C		.200	.071	.867	.048	.461	

WV	T <sub>av</sub>	P <sub>H<sub>2</sub>O</sub>	P <sub>H<sub>2</sub>O</sub>	P <sub>H<sub>2</sub>O</sub>	P <sub>H<sub>2</sub>O</sub>	n	T	A
<b>TYPE 2 (Condition B)</b> HEATED WITH SUPERHEATED H <sub>2</sub> O								
127A	180	.094	.040	.943	.010		811.2	7.48
B		.052	.028	.983	.011		792.0	6.21
C		.051	.028	.984	.011		788.0	6.60
128A	180	.127	.096	.917	.010		609.0	20.3
B		.120	.098	.908	.012		600.0	17.5
C		.131	.099	.906	.012		595.0	19.6
129A	180	.141	.127	.973	.023		338.0	108.0
B		.140	.113	.981	.023		330.0	79.6
C		.140	.143	.972	.019		342.2	127.8
130A	180	.088	.043	.927	.012		231.9	32.3
B		.092	.044	.920	.016		204.7	11.6
C		.095	.043	.917	.020		207.9	17.7
131A	215	.128	.083	.901	.026		320.0	21.1
B		.131	.088	.895	.030		300.0	22.3
C		.133	.088	.903	.021		313.0	23.1
132A	215	.045	.020	.986	.023		1135	2.60
B		.051	.032	.980	.016		1095	6.80
C		.046	.033	.989	.014		1093	6.30
133A	215	.208	.037	.976	.019		408.0	120.00
B		.210	.079	.970	.038		376.7	31.20
C		.205	.140	.981	.042		440.0	164.00
137A	215	.170	.090	.914	.070		242.1	18.0
B		.206	.080	.914	.077		189.9	13.6
C		.197	.082	.920	.072		209.4	15.2
147A	215	.196	.110	.903	.021		444.8	126.0
B		.275	.117	.905	.021		438.8	118.0
152A	280	.122	.048	.917	.086		158.0	19.1
B		.120	.046	.904	.044		140.0	26.3
C		.122	.083	.910	.079		176.1	26.1
157A	280	.216	.082	.909	.083		109.0	78.3
B		.212	.081	.909	.083		107.0	80.1
C		.209	.084	.904	.041		117.0	81.8
160A	280	.091	.086	.920	.023		218.0	10.1
B		.091	.082	.913	.079		275.0	17.6
C		.091	.084	.914	.028		213.2	10.8
170A	280	.043	.026	.998	.020		273.0	7.60
B		.040	.026	.997	.020		264.0	6.84
C		.041	.025	.999	.025		263.1	6.94
<b>TYPE 3</b>								
178A	180	.092	.043	.989	.026		1251	41.9
B		.094	.042	.989	.020		1747	60.3
C		.083	.074	.975	.040		458.0	114.0
<b>TYPE 10 (Condition A)</b> PIPING								
156A	180	.064	.042	.930	.018		339.0	3.04
B		.057	.041	.930	.018		407.4	3.57
C		.057	.041	.930	.018		378.4	3.71
156A	180	.094	.028	.977	.029		343.2	0.61
B		.094	.028	.979	.028		321.5	1.21
C		.094	.022	.979	.028		337.0	1.13
156A	215	.027	.026	.978	.028		273.0	1.52
B		.027	.024	.975	.028		271.5	1.27
C		.027	.024	.976	.029		280.9	1.80
151A	215	.042	.026	.941	.012		439.0	5.46
B		.043	.027	.940	.012		467.7	6.76
C		.043	.026	.938	.014		389.0	5.52
156A	280	.027	.025	.970	.028		309.5	1.42
B		.028	.026	.970	.029		308.0	1.42
C		.027	.028	.970	.028		304.1	1.40
156A	280	.053	.047	.943	.017		443.7	4.78
B		.054	.044	.944	.017		430.9	5.61
C		.052	.044	.943	.017		433.2	5.28
<b>TYPE 10 (Condition B)</b> HEATED WITH SUPERHEATED H <sub>2</sub> O								
160A	180	.049	.029	.955	.028		344.0	4.11
B		.049	.029	.956	.028		362.3	4.08
C		.071	.041	.952	.031		286.0	4.10
167A	180	.029	.028	.994	.027		299.0	1.27
B		.029	.028	.993	.027		273.6	1.44
C		.028	.029	.995	.027		272.7	1.44
166A	215	.039	.028	.989	.027		337.0	1.72
B		.038	.028	.993	.026		336.5	1.70
C		.038	.025	.995	.028		328.0	1.70
166A	215	.042	.030	.954	.014		332.7	4.49
B		.042	.032	.950	.013		325.5	4.71
C		.040	.031	.957	.015		329.9	4.71
166A	280	.032	.024	.944	.020		191.6	5.08
B		.032	.027	.944	.020		198.0	4.91
C		.032	.027	.945	.020		302.2	5.08
166A	280	.028	.028	.994	.027		359.0	2.88
B		.028	.028	.994	.027		358.2	2.70
C		.027	.028	.994	.027		382.9	2.81

WV	T <sub>av</sub>	P <sub>H<sub>2</sub>O</sub>	P <sub>H<sub>2</sub>O</sub>	P <sub>H<sub>2</sub>O</sub>	P <sub>H<sub>2</sub>O</sub>	n	T	A
<b>TYPE 10 (Condition C)</b> HEATED WITH SUPERHEATED H <sub>2</sub> O								
176A	180	.064	.042	.950	.026		263.0	5.76
B		.064	.041	.954	.026		247.0	5.13
C		.069	.040	.960	.026		263.1	5.99
176A	180	.020	.020	.997	.027		303.1	1.98
B		.028	.020	.990	.027		280.0	2.02
C		.028	.020	.996	.027		303.1	2.13
176A	215	.027	.021	.980	.028		323.1	2.09
B		.026	.021	.984	.028		320.0	1.97
C		.027	.020	.988	.028		320.0	2.28
176A	215	.042	.048	.906	.011		190.0	5.20
B		.044	.044	.902	.012		177.0	5.67
C		.042	.039	.931	.016		138.0	4.90
176A	280	.052	.040	.960	.015		212.0	6.07
B		.053	.027	.955	.018		211.0	5.04
C		.053	.035	.957	.017		218.0	6.24
177A	280	.027	.019	.988	.011		197.7	2.66
B		.026	.018	.986	.009		199.0	2.28
C		.028	.018	.984	.009		195.0	2.41
<b>TYPE 11 (Condition A)</b> PIPING								
146A	180	.043	.049	.912	.018		386.0	1.94
B		.044	.040	.931	.028		384.0	2.40
C		.045	.048	.930	.028		384.2	3.07
141A	180	.028	.027	.978	.027		410.0	.79
B		.026	.027	.978	.021		420.0	.80
C		.028	.027	.977	.028		398.0	.94
157A	215	.028	.028	.980	.017		113.0	6.54
B		.028	.028	.980	.013		121.0	3.88
C		.029	.028	.948	.018		100.0	3.40
140C	215	.029	.027	.976	.027		432.0	1.51
B		.029	.028	.972	.027		436.0	1.51
A		.028	.028	.976	.027		420.0	1.08
150C	280	.027	.028	.978	.027		407.7	1.78
B		.027	.028	.978	.027		410.0	1.42
A		.027	.028	.979	.027		412.0	1.24
150A	280	.040	.042	.904	.014		350.0	4.1
B		.041	.043	.946	.019		375.0	4.21
C		.050	.043	.948	.017		391.7	4.57
<b>TYPE 11 (Condition B)</b> HEATED WITH SUPERHEATED H <sub>2</sub> O								
164A	180	.043	.040	.940	.010		149.0	3.79
B		.046	.041	.945	.010		149.0	3.97
C		.047	.043	.945	.008		141.0	3.62
173A	180	.031	.027	.978	.028		180.0	1.20
B		.031	.028	.977	.027		191.0	1.72
C		.030	.028	.979	.027		190.7	1.57
172A	215	.032	.026	.978	.027		301.0	1.87
B		.031	.025	.977	.027		191.0	1.84
C		.030	.024	.979	.027		186.0	1.82
166A	215	.040	.048	.947	.012		259.0	4.28
B		.039	.047	.947	.013		258.7	4.71
C		.038	.048	.949	.012		271.0	4.47
171A	280	.029	.019	.984	.028		115.2	1.81
B		.029	.019	.979	.021		118.0	1.87
C		.030	.021	.984	.029		145.7	2.00
170A	280	.040	.030	.950	.020		128.0	3.45
B		.040	.031	.950	.018		130.7	3.32
C		.048	.033	.955	.019		116.0	3.24
<b>TYPE 12 (Condition A)</b> PIPING HEATED WITH H <sub>2</sub> O								
140A	215	.082	.044	.942	.013		307.7	4.20
B		.058	.045	.941	.013		342.1	4.50
C		.058	.046	.941	.013		361.6	4.13
D		.052	.046	.942	.013		364.0	4.37
<b>TYPE 12 (Condition B)</b> HEATED WITH H <sub>2</sub> O								
148A	215	.042	.037	.971	.019		479.0	20.40
B		.042	.038	.970	.020		476.1	20.40
C		.043	.038	.968	.020		484.2	20.60
D		.042	.038	.969	.020		477.0	20.20
<b>TYPE 13 (Condition A)</b> PIPING HEATED WITH H <sub>2</sub> O								
171A	215	.048	.026	.945	.020		467.0	21.71
B								



**TABLE 26**  
PTFE TUBE TREATED WITH  $H_2O_2$

207A	215	.040	.047	.042	.014	.1197	1.28	504
B		.040	.047	.042	.014	.1197	1.70	
C		.040	.047	.042	.014	.1197	1.20	

**TABLE 27**  
SILICA TUBE TREATED WITH  $H_2O_2$

208A	215	.038	.032	.078	.009	.2319	1.03	504
B		.038	.032	.078	.010	.2118	1.13	
C		.038	.030	.078	.010	.2054	1.24	

**TABLE 28**

210A	715	.060	.061	.042	.015	.2145	2.30	504
B		.060	.060	.042	.015	.2018	2.20	
C		.060	.060	.042	.015	.2028	2.18	

**TABLE 29**  
PTFE COATED WITH 5% CLORED MPTYL SILANE

211A	715	.060	.060	.042	.015	.2018	2.20	502
B		.060	.060	.042	.015	.2028	1.99	
C		.060	.060	.042	.015	.2158	1.99	

**TABLE 30**  
PTFE COATED WITH 5% MPTYL METHACRYLATE

212A	120	.077	.047	.043	.008	.2898	11.65	500
B		.070	.047	.043	.008	.2827	8.86	
C		.060	.040	.040	.008	.2889	8.00	

**TABLE 31**  
PTFE TREATED WITH  $H_2O_2$

277A	215	.076	.028	1.000	.008	.3758	2.38	502
B		.036	.028	.998	.010	.2928	1.94	
C		.028	.028	.998	.010	.4728	1.81	

**TABLE 32**

278A	715	.081	.070	.047	.015	.2523	6.37	500
B		.081	.076	.034	.013	.2779	7.50	
C		.088	.074	.038	.013	.2600	6.78	

**TABLE 33**  
PTFE COATED WITH 5% BCI

282A	715	.078	.058	.043	.013	.2892	7.08	502
B		.075	.058	.038	.014	.2876	6.78	
C		.073	.057	.035	.013	.2844	6.41	

**TABLE 34**

284A	215	.034	.025	.993	.009	.1175	2.16	502
B		.038	.030	.991	.010	.1188	2.26	
C		.037	.028	.994	.008	.1193	2.14	

**TABLE 35**  
PTFE TREATED WITH 1% SW

285A	215	.027	.026	1.000	.007	.2888	1.64	502
B		.027	.026	1.008	.008	.2841	1.88	
C		.027	.026	1.001	.008	.2797	1.63	

**TABLE 36**

286A	215	.048	.044	.988	.010	.4628	3.61	502
B		.070	.044	.934	.010	.4867	4.29	
C		.072	.047	.931	.011	.4828	4.08	

**TABLE 37**  
PTFE TREATED WITH  $H_2O_2$  HEATED TO 400-450°C FOR 2 HOURS

279A	215	.057	.040	.040	.010	.2828	6.58	502
B		.048	.044	.038	.009	.2844	6.75	
C		.070	.048	.038	.010	.2813	6.78	

**TABLE 101 (Condition A)**  
PTFE TREATED WITH  $H_2O_2$

207A	215	.042	.038	.040	.014	.1843	2.07	502
B		.043	.038	.040	.018	.1718	2.51	
C		.041	.032	.040	.018	.1841	2.41	

**TABLE 102**

208A	180	.034	.038	.078	.014	.1448	1.87	502
B		.034	.038	.078	.018	.1348	1.97	
C		.038	.038	.078	.018	.1815	1.92	

**TABLE 103**

209A	180	.038	.038	.078	.017	.1858	1.88	502
B		.032	.038	.078	.017	.1828	1.74	
C		.032	.037	.077	.017	.1899	1.68	

**TABLE 104**

210A	117	.038	.032	.078	.018	.2844	2.80	502
B	122	.038	.032	.078	.018	.2870	1.90	
C	118	.038	.030	.078	.017	.3019	2.33	

**TABLE 105**

276A	121	.104	.104	.048	.008	.2882	5.77	501
B		.108	.108	.047	.008	.2854	7.42	
C		.103	.103	.044	.008	.2824	6.84	

**TABLE 106**

281A	189	.034	.034	.018	.018	.3391	3.15	502
B	110	.034	.034	.018	.017	.3609	3.47	
C	111	.034	.034	.018	.018	.3243	3.12	

**TABLE 107**

276A	110(116)	.088	.048	.038	.008	.2864	6.28	502
B	110(117)	.098	.048	.038	.009	.4058	8.86	
C	110(116)	.090	.048	.037	.010	.2894	5.27	

**TABLE 101 (Condition B)**  
PTFE

279A	715	.067	.087	.031	.013	.2804	4.11	502
B		.089	.088	.047	.014	.2771	5.03	
C		.084	.087	.049	.014	.2843	4.87	

**TABLE 102**

282A	215	.041	.037	.078	.009	.3709	2.36	502
B		.038	.038	.042	.007	.4393	2.18	
C		.038	.038	.043	.008	.4351	2.01	

**TABLE 101 (Condition C)**  
SOFT GLASS ROD (A = 256 mm) ADDED TO PTFE 101

279A	215	.045	.048	.043	.011	.2816	11.8	204
B		.073	.051	.043	.015	.2152	19.8	
C		.045	.049	.040	.014	.2834	14.8	

**TABLE 103**

279A	215	.042	.038	.040	.012	.2542	1.32	204
B		.048	.034	.047	.007	.3028	.98	
C		.037	.038	.042	.008	.2807		

**TABLE 101 (Condition D)**  
SOFT GLASS ROD TREATED WITH  $H_2O_2$

281A	215	.038	.038	.048	.008	.3378	1.42	4
B		.038	.038	.048	.009	.3031	1.28	
C		.038	.038	.048	.011	.3148	1.72	

**TABLE 102**

286A	215	.043	.044	.044	.012	.3784	2.89	204
B		.048	.047	.040	.013	.3743	1.11	
C		.043	.048	.048	.013	.3887	2.25	

**TABLES**

**TABLE 27 (Condition A)**  
EMPTY PTFE TUBE FOR PTFE 219 - 311

201A	150	.018	.017	.042	.009	.2810	1.87	162
B		.018	.017	.044	.006	.2819	1.87	
C		.018	.016	.040	.009	.2829	1.98	

**TABLE 28**

202A	180	.044	.044	.041	.018	.2141	4.02	162
B		.048	.046	.030	.018	.2143	6.98	
C		.044	.042	.041	.013	.2143	4.48	

**TABLE 27 (Condition B)**  
EMPTY PTFE TUBE FOR PTFE 212 - 288

212A	150	.039	.039	.043	.008	.2834	7.04	162
B		.039	.039	.048	.004	.2710	1.88	
C		.039	.038	.048	.004	.2855	2.99	

**TABLE 29**

214A	150	.078	.073	.044	.008	.2080	4.06	162
B		.074	.078	.044	.008	.2136	4.32	
C		.078	.071	.048	.008	.2072	5.28	

**TABLE 30**

222A	180	.126	.127	.044	.008	.2026	15.2	162
B		.126	.127	.047	.004	.2084	14.8	
C		.125	.126	.049	.008	.2181	14.0	

**TABLE 27 (Condition B)**  
(Continued)

222A	180	.178	.171	.041	.008	.2889	12.1	162
B		.182	.173	.048	.008	.2951	15.0	
C		.188	.174	.037	.004	.2954	16.1	

**TABLE 31**

226A	180	.129	.125	.028	.006	.2814	47.1	162
B		.124	.128	.028	.006	.2721	48.3	
C		.124	.122	.030	.008	.2745	47.8	

**TABLE 32**

218A	180	.043	.040	.078	.008	.2580	4.43	162
B		.044	.043	.078	.008	.2621	5.71	
C		.044	.042	.077	.008	.2741	4.45	

**TABLE 33**

217A	180	.074	.068	.040	.008	.2889	8.03	162
B		.073	.068	.048	.007	.2809	7.47	
C		.078	.068	.048	.008	.2898	8.14	

**TABLE 34**

228A	180	.157	.140	.047	.004	.2075	23.2	162
B		.153	.139	.072	.004	.2088	25.9	
C		.144	.134	.073	.004	.2096	17.9	

**TABLE 35**

221A	180	.188	.182	.040	.008	.2269	29.1	162
B		.184	.180	.048	.008	.2211	29.1	
C		.188	.183	.040	.008	.2108	24.7	



METALS AT 120°C

NO	T <sub>av</sub>	P <sub>H<sub>2</sub>O</sub> <sup>1</sup>	P <sub>H<sub>2</sub>O</sub> <sup>0</sup>	P <sub>H<sub>2</sub>O</sub> <sup>2</sup>	P <sub>O<sub>2</sub></sub>	B	B	A	T
STAINLESS STEEL 316									
CONDITION A (REPRODUCIBLE)									
AREA OF GLASS = 162 cm <sup>2</sup>									
AREA OF TOTAL BED = 12.98 cm <sup>2</sup>									
306A	120	.001	.040	.075	.012	.0041	9.15	1.25	
B		.002	.038	.079	.015	.0135	9.43		
C		.003	.036	.081	.020	.0032	8.77		
307A	120	.000	.030	.071	.012	.0022	17.69	2.90	
B		.002	.028	.070	.012	.0019	19.18		
308A	120	.006	.001	.003	.001	.0167	7.04	2.75	
B		.004	.000	.000	.001	.0179	6.43		
C		.004	.000	.000	.001	.0187	6.11		
STAINLESS STEEL 303									
CONDITION A (REPRODUCIBLE)									
AREA OF GLASS = 162 cm <sup>2</sup>									
AREA OF TOTAL BED = 12.98 cm <sup>2</sup>									
303A	120	.005	.004	.000	.000	.0069	9.92	1.25	
B		.005	.000	.000	.000	.0102	10.78		
C		.005	.003	.000	.000	.0073	10.11		
304A	120	.000	.000	.001	.000	.0156	9.59	2.90	
B		.000	.000	.001	.000	.0090	9.68		
305A	120	.001	.002	.004	.001	.0105	1.09	2.75	
B		.001	.002	.004	.001	.0118	1.00		
C		.004	.003	.006	.001	.0042	4.77		
STAINLESS STEEL 304									
CONDITION A (REPRODUCIBLE)									
AREA OF GLASS = 162 cm <sup>2</sup>									
AREA OF TOTAL BED = 12.98 cm <sup>2</sup>									
304A	120	.003	.043	.055	.018	.0034	10.33	1.5	
B		.004	.040	.051	.016	.0040	10.2		
C		.002	.042	.055	.016	.0039	10.4		
305A	120	.000	.045	.050	.018	.0073	20.4	2.5	
B		.000	.045	.050	.016	.0070	18.4		
C		.000	.040	.050	.016	.0081	24.9		
306A	120	.000	.000	.000	.000	.0112	4.7	3.75	
B		.000	.000	.000	.000	.0107	3.8		
307A	120	.000	.004	.000	.000	.0157	11.2	5.0	
B		.000	.004	.000	.000	.0121	11.9		
C		.000	.007	.000	.000	.0149	11.7		
308A	120	.000	.000	.000	.000	.0043	13.7	6.0	
B		.000	.000	.000	.000	.0075	13.7		
C		.000	.000	.000	.000	.0073	13.0		
309A	120	.000	.000	.000	.000	.0132	3.06	7.50	
B		.000	.000	.000	.000	.0117	3.62		
C		.000	.000	.000	.000	.0108	3.04		

NO	T <sub>av</sub>	P <sub>H<sub>2</sub>O</sub> <sup>1</sup>	P <sub>H<sub>2</sub>O</sub> <sup>0</sup>	P <sub>H<sub>2</sub>O</sub> <sup>2</sup>	P <sub>O<sub>2</sub></sub>	B	B	A	T
STAINLESS STEEL 303									
CONDITION B (REPRODUCIBLE)									
AREA OF GLASS = 162 cm <sup>2</sup>									
AREA OF TOTAL BED = 12.98 cm <sup>2</sup>									
303A	120	.004	.046	.065	.013	.0003	14.5	1.45	
B		.003	.044	.065	.014	.0084	14.6		
C		.001	.040	.066	.014	.0045	13.3		
304A	120	.000	.030	.082	.016	.0080	7.72	2.90	
B		.000	.032	.078	.019	.0124	7.81		
C		.000	.021	.080	.019	.0167	7.60		
305A	120	.000	.004	.084	.021	.0114	6.36	2.75	
B		.000	.003	.086	.024	.0081	6.34		
C		.000	.003	.087	.022	.0082	6.28		
STAINLESS STEEL 303									
CONDITION C (REPRODUCIBLE)									
AREA OF GLASS = 162 cm <sup>2</sup>									
AREA OF TOTAL BED = 12.98 cm <sup>2</sup>									
303A	120	.004	.040	.068	.013	.0047	12.41	1.45	
B		.002	.048	.065	.013	.0093	11.0		
C		.000	.047	.070	.014	.0041	11.0		
304A	120	.000	.037	.079	.016	.0003	7.77	2.90	
B		.000	.036	.080	.017	.0003	7.87		
C		.000	.036	.081	.016	.0003	7.90		
305A	120	.000	.000	.084	.019	.0150	6.64	2.75	
B		.000	.000	.087	.019	.0103	6.71		
C		.000	.000	.087	.018	.0037	7.12		
STAINLESS STEEL 304									
CONDITION A (REPRODUCIBLE)									
AREA OF GLASS = 162 cm <sup>2</sup>									
AREA OF TOTAL BED = 12.98 cm <sup>2</sup>									
303A	120	.000	.051	.044	.016	.0007	3.06	1	
303B	120	.000	.000	.041	.016	.0070	7.22	2	
304A	120	.000	.032	.059	.011	.0072	4.07	3	
303C	120	.000	.000	.063	.019	.0029	4.07	4	
305A	120	.000	.000	.039	.012	.0074	11.9	5	
B		.000	.000	.069	.013	.0091	11.43		
C		.000	.000	.031	.014	.0019	11.68		
306A	120	.000	.042	.036	.014	.0121	7.15	7	
B		.000	.039	.036	.012	.0120	6.40		
C		.000	.036	.034	.015	.0160	7.31		
307A	120	.000	.045	.032	.017	.0045	16.9	8	
B		.000	.048	.030	.015	.0014	17.0		
C		.000	.048	.031	.018	.0007	16.88		
308A	120	.000	.000	.048	.015	.0003	6.09	9	
B		.000	.000	.049	.016	.0003	6.84		
C		.000	.000	.047	.013	.0003	5.21		

NON-REPRODUCIBLE RUNS

NO	T <sub>av</sub>	P <sub>H<sub>2</sub>O</sub> <sup>1</sup>	P <sub>H<sub>2</sub>O</sub> <sup>0</sup>	P <sub>H<sub>2</sub>O</sub> <sup>2</sup>	P <sub>O<sub>2</sub></sub>	B	B	A	T
TYPE 303									
303A	460	.020	.113	.062	.000	.0005	47.6	392	300
B		.006	.011	.044	.004	.0013	43.6		
303B	427	.028	.010	.038	.003	.0018	25.7	392	300
B		.028	.000	.063	.000	.0004	31.0		
C		.029	.001	.037	.004	.0009	22.2		
303C	477	.000	.000	.039	.001	.0005	18.7	392	300
B		.026	.000	.060	.000	.0003	12.2		
C		.001	.000	.037	.001	.0003	14.1		
303D	765	.000	.000	.000	.000	.0000	12.7	392	300
B		.000	.000	.000	.000	.0000	18.2		
C		.000	.000	.000	.000	.0000	15.6		
303E	329	.000	.000	.000	.000	.0000	10.3	392	300
B		.000	.000	.000	.000	.0000	10.6		
C		.000	.000	.000	.000	.0000	13.3		
303F	290	.000	.000	.000	.000	.0000	6.2	392	300
B		.000	.000	.000	.000	.0000	7.1		
C		.000	.000	.000	.000	.0000	5.1		
303G	280	.000	.000	.000	.000	.0000	3.3	392	300
B		.000	.000	.000	.000	.0000	1.8		
C		.000	.000	.000	.000	.0000	0.8		
TYPE 304									
304A	450	.004	.011	.033	.008	.0003	117.7	392	300
B		.002	.010	.030	.007	.0000	149.1		
C		.002	.011	.041	.004	.0006	119.5		
304B	460	.002	.010	.030	.005	.0000	36.2	392	300
B		.002	.010	.031	.008	.0000	22.2		
C		.006	.009	.037	.007	.0000	20.9		
TYPE 308									
308A	490	.000	.001	.000	.000	.0000	46.52	392	300
B		.000	.000	.000	.000	.0000	59.47		
C		.000	.000	.000	.000	.0000	52.7		
308B	480	.000	.000	.000	.000	.0000	49.4	392	300
B		.000	.000	.000	.000	.0000	50.4		
C		.000	.000	.000	.000	.0000	45.1		
308C	470	.000	.000	.000	.000	.0000	55.2	392	300
B		.000	.000	.000	.000	.0000	55.8		
C		.000	.000	.000	.000	.0000	58.5		
308D	460	.000	.000	.000	.000	.0000	52.5	392	300
B		.000	.000	.000	.000	.0000	54.4		
C		.000	.000	.000	.000	.0000	55.2		
308E	440	.000	.000	.000	.000	.0000	41.3	392	300
B		.000	.000	.000	.000	.0000	41.7		
C		.000	.000	.000	.000	.0000	41.3		
308F	400	.000	.000	.000	.000	.0000	27.6	392	300
B		.000	.000	.000	.000	.0000	28.3		
C		.000	.000	.000	.000	.0000	33.9		
308G	360	.000	.000	.000	.000	.0000	10.7	392	300
B		.000	.000	.000	.000	.0000	8.8		
C		.000	.000	.000	.000	.0000	1.4		
308H	310	.000	.000	.000	.000	.0000	1.9	392	300
B		.000	.000	.000	.000	.0000	1.1		
C		.000	.000	.000	.000	.0000	2.0		

was treated with acid, fused, treated with sodium hydroxide and finally coated with boric oxide. Tubes 8 and 9 prior to being coated were unaltered Pyrex surfaces. Condition A of tube 9 refers to its behaviour immediately after receiving the boric oxide coating. It was then exposed to the atmosphere for four days, which condition was designated condition B. Next a bundle of Pyrex rods, coated with a fused boric oxide coating, were added to tube 9 in order to change the surface to volume ratio. The area of the tube was 590 cm<sup>2</sup>, that of rods plus tube was 1450 cm<sup>2</sup>. The rate data in Figure 3 are based on the total area, indicating that the activity of the packing was slightly greater than that of the tube. After the tube was studied in this condition for a period of about one week, these rods were removed, which condition was designated as condition D.

As the boric oxide surface continued to be exposed to hydrogen peroxide vapor there occurred an initial increase in surface activity, but after this initial aging, the activity remained constant. Thus, some 20 hours of exposure to H<sub>2</sub>O<sub>2</sub> vapor elapsed between conditions B and D of tube 9, yet the activity is seen to be the same. Surfaces exposed to hydrogen peroxide vapor for but a short period, [tubes 7 (in condition F), 8 and 9 (in condition A), --all shown on Figure 3] have approximately equal activities.

The rate of decomposition of hydrogen peroxide vapor at 215°C on a fused silica (Vitreosil) surface, tube 27, which had been treated with an acid, and also on a Vycor surface, tube 11 (in condition A), can be seen on Figure 4. In Figure 5 are the results of a study of the decomposition on a soft glass surface. The soft glass surface studied was a rod which was placed coaxially in a Pyrex tube, tube 101, and rested on supports blown in this tube. (The data in Figure 5 are calculated for the area of soft glass exposed, after allowing for the extent of reaction on Pyrex). Eight different Pyrex surfaces were examined and the results are to be seen on Figure 6. Finally a lead glass surface, tube 20, was studied and the results are in Figure 7.

To summarize and compare the above results, the rates of decomposition observed on the various glass surfaces are tabulated below for a partial pressure of hydrogen peroxide of 0.04 atm. The temperature for all the studies was 215°C.

Table II  
 RATES OF DECOMPOSITION ON SEVERAL GLASSES

Temp. = 215°C.

Surface	Composition in Wt. %						Rates of decomp. (mole/min cm <sup>2</sup> ) x 10 <sup>6</sup> P <sub>H<sub>2</sub>O<sub>2</sub></sub> = 0.04 atm.	
	SiO <sub>2</sub>	B <sub>2</sub> O <sub>3</sub>	Na <sub>2</sub> O	K <sub>2</sub> O	CaO	Al <sub>2</sub> O <sub>3</sub>		PbO
Fused Silica	100							2
Boric Oxide		100						2.5-4
Vycor	96	4	0.02			0.04		2.7
Pyrex	80.5	12.9	3.8	0.4		2.2		3-6
Soft Glass	70		14	6.2	6.3	3.3		9
Lead Glass	68		10	6.0	1		15	43

Although there is considerable quantitative irreproducibility, it is evident that the activities of the different glasses rank as follows: Fused Silica < Boric oxide ≈ Vycor < Pyrex < Soft Glass << Lead glass.

The relationship in Table II between the compositions of these surfaces and their catalytic activity suggests that sodium, potassium, calcium, aluminum and especially lead atoms in the glass are active centers for the decomposition. Dowden (7) has suggested that for electron transfer reactions, the electrical properties of the material are informative as to a catalyst's activity. It is interesting that a ranking of these 5 glasses in order of increasing dielectric constant is the same as their ranking in order of increasing catalytic activity, although this may be fortuitous.

#### Ion Addition to Pyrex

To test further the hypothesis that the catalytic activity of a glass surface is a function of the sodium in the glass, two Pyrex tubes were soaked in 5% sodium hydroxide, which presumably reacts with the glass to form Si-O-Na bonds on the surface (35). The decomposition rate on these surfaces can be seen on Figure 8. Tube 7 was soaked for 16 hours (this is designated condition E) and tube 24, for 2 hours, (called condition A). It can be seen that this treatment of tube 7 increased its activity about threefold.

In addition to sodium, two other substances--silver and iron--were added to Pyrex by treating the glass for 20 hours with a 1N nitrate solution of these ions at 60°C. These ions may add to the surface by an exchange mechanism with existing ions in the glass (8,12) or they may be reduced to a lower oxidation state on the surface. In the latter case an ion may acquire an electron at a surface defect or else it could rearrange its electronic field as

it approaches the glass surface (36). For example, the electrons of the polar silver ion are repelled by the glass so that in the direction of the glass the silver behaves as  $Ag^{+2}$ , whereas in the opposite direction the chemical properties of the surface resemble those of metallic silver.

The determination of the catalytic activity of a surface after the addition of ions gives no measure of the activities of individual sites since their number is unknown. Consequently to determine which of two elements on a surface is the more reactive, a Pyrex tube was first immersed in a solution of one of the species and the rate of decomposition measured; then the tube was immersed in the other species and the rate of decomposition again determined. This procedure was then repeated in the reverse order in a second Pyrex tube. In each case the tube was immersed in a 1N solution of the appropriate nitrate salt for 20 hours at 60°C.

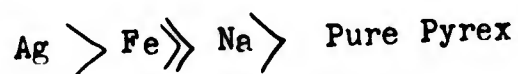
On Figure 9 is shown a comparison of sodium and silver. Tube 12 was first treated with sodium nitrate, (designated as condition A) and then with silver nitrate, condition B. Tube 13 was treated first with silver nitrate, condition A, followed by the sodium nitrate treatment, condition B. The silver is seen to be more reactive than sodium. Because subsequent treatment with sodium nitrate of a surface previously treated with silver nitrate (tube 13) did not greatly lower the activity, it appears that the silver exists not as an ion on the surface, but rather in the reduced metallic state.

The effect of treating a Pyrex surface with sodium and ferric nitrates was compared in the same way, the results being shown on Figure 10. Pyrex tube 14 was first treated with ferric nitrate, (condition A), and then treated with sodium nitrate, (condition B). Tube 15 was given the reverse treatment. The results indicate that a iron active center is more reactive than a sodium center. Because the sodium did not significantly replace the iron, it appears likely that the iron was adsorbed in a reduced form, similar to that occurring with silver.

A comparison of silver and iron is shown in Figure 11. Tube 16 in condition A was a Pyrex tube treated with silver nitrate and condition B was this same tube after ferric nitrate treatment. Tube 17 was a Pyrex tube treated first with ferric nitrate and then with silver nitrate. These results indicate that silver active sites are more reactive than iron.

### Summary

The presence of cations on a glass surface increases the catalytic activity for the heterogeneous decomposition of hydrogen peroxide vapor. The activities of these individual sites rank as follows:



The presence of lead in a glass greatly increased the catalytic nature of a glass. The activities of these substances for the decomposition rate of hydrogen peroxide vapor parallel their activities for the decomposition of the liquid. Thus, silver, lead and ferrous ions are excellent catalysts for the decomposition of liquid  $H_2O_2$ , whereas sodium ions are relatively poor.

### Acid Treatment of Pyrex

The preceding results indicate that cations on a glass surface are active centers and that if these were removed, the resulting surface would be more inert. One method is by treatment with an acid (24), which replaces them with hydrogen ions by an ion exchange mechanism. However, the silica network is also attacked, thereby forming a surface resembling silica gel. Because of this double action, it is desirable to determine the effect of different types and concentrations of acids.

Figure 12 shows the activities of several Pyrex tubes which were treated with nitric acid. Tubes 18, 10 and 7 were soaked for 20 hours in concentrated (15.5N) nitric acid, while tubes 6 and 19 were treated with 2N nitric acid for the same period of time. All these tubes had been exposed to  $H_2O_2$  vapor in the studies reported in Figure 6 before being subjected to acid treatment. The kind of treatment with  $HNO_3$  is evidently less important than adventitious variation from sample to sample of Pyrex. Figure 13 shows the rates of decomposition observed on several Pyrex tubes which had been soaked for 20 hours in 4N phosphoric acid. In Figure 14 are the rates of decomposition on Pyrex surfaces previously treated with 4N hydrochloric or 4N sulfuric acids (tubes 33 and 34) or with 1% hydrofluoric acid for 20 hours.

### Summary

In Table III are tabulated the rates of reaction at 215°C on the various acid treated tubes and also the rates of reaction on some of the untreated surfaces. It is concluded that acid treatment decreases the activity of the surfaces, and that 4N phosphoric acid and 2N nitric acid are the most satisfactory acid solutions with which to treat Pyrex.

Table III  
SUMMARY OF ACID-TREATED PYREX SURFACES  
T = 215°C

<u>Tube</u>	Rate of Decomposition x 10 <sup>6</sup> (moles/min cm <sup>2</sup> ), at P <sub>H<sub>2</sub>O<sub>2</sub></sub> = 0.04 atm.	
	<u>Treated</u>	<u>Untreated</u>
2N HNO <sub>3</sub>		
Tube 6 (in condition B)	1	5.2
Tube 19 (in condition B)	1.9	6.5
Conc. HNO <sub>3</sub>		
Tube 18 (in condition B)	3.75	6.5
Tube 10 (in condition C)	3.75	
Tube 7 (in condition B)	1	2.5
4N H <sub>3</sub> PO <sub>4</sub>		
Tube 22 (in condition B)	1.75	3.5
Tube 25 (in condition A)	1.75	
Tube 26 (in condition A)	1.1	
Tube 101 (in condition A)	2.75	
4N H <sub>2</sub> SO <sub>4</sub>		
Tube 34	3.25	
4N HCl		
Tube 33	3.25	
1% HF		
Tube 35	2.3	

There is considerable irreproducibility of results, even where two tubes were taken from the same original stock of glass, and treated in exactly the same manner, as for example tubes 25 and 26, treated with H<sub>3</sub>PO<sub>4</sub>.

#### Acid Treatment of Various Types of Glasses

The effects of acid treatment of other glass surfaces are shown on Figures 15 and 16, and are summarized in Table IV. The Vycor was treated with 2N nitric acid for 20 hours; the fused silica, soft glass and lead glasses were treated with 4N phosphoric acid.

Table IV

## EFFECT OF ACID TREATMENT ON VARIOUS TYPES OF GLASSES

T = 215°C

Rate of Decomposition x 10<sup>6</sup>  
(moles/min cm<sup>2</sup>), at P<sub>H<sub>2</sub>O<sub>2</sub></sub> = 0.04 atm

<u>Surface</u>	<u>Before Acid Treatment</u>	<u>After Acid Treatment</u>
Fused Silica		2
Pyrex (tube 22)	3.7	1.75
Vycor	2.7	3
Soft Glass	9	2
Lead Glass	43	25

The above summary emphasizes the fact that as the cations are removed from the glass surfaces, the activities converge towards a common value which presumably is the activity of silica. The seeming slight increase in the catalytic activity of Vycor is within experimental accuracy. The activity of lead glass was not decreased as much as the others, presumably because all of the lead atoms, which are bound more securely to the silica network than are the other substances, were not entirely removed by the action of the acid.

Miscellaneous Treatments

Sodium Stannate - Sodium stannate (Na<sub>2</sub>SnO<sub>3</sub>·3H<sub>2</sub>O) stabilizes liquid hydrogen peroxide solutions by hydrolyzing to form colloidal hydrous stannic oxide (SnO<sub>2</sub>·xH<sub>2</sub>O)(30) which absorbs catalytic ions, either in solution or on vessel surfaces. A Pyrex surface, previously acid-treated, was soaked in a 200 p.p.m. sodium stannate solution for 20 hours. The results on Figure 17 indicate that this treatment slightly increased the tube activity.

Sulfur Dioxide - The sodium ions in glass have been reported to react with gaseous sulfur dioxide to form sulfate type structures (5,6). To see if this treatment would poison the active centers, gaseous sulfur dioxide at 200°C was passed for 20 hours through a Pyrex tube which had been previously treated with 5% sodium hydroxide solution, tube 24 (in condition A). On Figure 18 it can be seen that the activity of the surface was not appreciably changed by this treatment.

Hydrogen Peroxide Solution - The common procedure for passivating surfaces which are to be used in contact with hydrogen peroxide liquid is to soak them in a hydrogen peroxide solution. However an acid-treated Pyrex tube, tube 18 (in condition B) after soaking for 20 hours in a 50% hydrogen peroxide solution showed no lowering of surface activity (see Figure 19).

Metakaolin - When a glass surface is heated at 300°C in contact with a slip of metakaolin, the hydrogen ions in the clay presumably replace the sodium ions in the glass by an ion exchange mechanism (37). A Pyrex tube, tube 10 in condition A, was treated in this manner, but as seen on Figure 20, the activity was unaffected.

Fused Surfaces - When a glass is heated to a temperature approaching the annealing temperature, the surface of the glass becomes more plane as the mechanical and intrinsic defects on the surface are eliminated. Figure 21 shows that a fused Pyrex surface is quite inert, about 10 times less reactive than an acid-treated Pyrex surface. Tube 103 was heated uniformly in a constant temperature bath to 490°C and was then cooled to 400°C in a time period of about 4 hours. Tube 100, on the other hand, was heated in the bath to 460°C, the temperature of which was lowered over a period of two hours to 250°C. The lowest temperature studied in this tube was 250°C; consequently, the datum point on this plot was extrapolated to 215°C.

Numerous attempts were made to fuse a surface with a small flame because such a method would be of greater ease in practical use. Tube 6, (in condition B), an acid treated Pyrex tube, was heated with a torch until the yellow sodium flame appeared. The temperature of Pyrex at this point is just below the annealing point, which is about 500°C. The torch was played up and down the surface so that the tube was at this temperature for approximately one minute. The activity of the resulting surface, designated as tube 6 in condition C, is shown on Figure 22 to be unaffected. On Figure 23 is the result of treating a second tube, tube 7 in condition B, in a similar manner as tube 6 with the exception that the flame was passed through the tube, thereby heating directly the catalytic surface. This likewise did not decrease the activity. A third Pyrex tube, tube 101 in condition A, was heated in the same manner as tube 6, but for a duration of 2 to 3 minutes. As is seen on Figure 24, the activity was not lowered.

All of these attempts were unsuccessful presumably because the glass surfaces were not heated and cooled uniformly. The defects which may have been removed, probably reappeared as the surface was cooled unevenly.

A Pyrex tube, tube 26, was heated to 430°C in a molten salt bath for half an hour. It is seen on Figure 24 that this did not decrease the rate of decomposition on the surface. The temperature and duration of heating were presumably insufficient to fuse the surface.

These results indicate that defects in a glass surface, which are electron donor sites (7, 25), are active sites for the decomposition of hydrogen peroxide vapor. When the defects are removed by fusing a surface, and the ions are removed by acid treatment, the activity of Pyrex is decreased by a factor of about 40.

### Activation Energy

On many of the surfaces decomposition rates were measured over a moderate temperature range. On Figure 26 is plotted the logarithm of the observed decomposition rate as calculated for a partial pressure of hydrogen peroxide of 0.04 atm., against the reciprocal of the absolute temperature. Also listed are the activation energies corresponding to the slopes of the lines.

It is seen the activation energies are small; change in temperature from 180°C to 250°C, for example, increases the reaction rate by a factor of only 2 or 3. Although the rate of reaction at a given temperature varies by a factor of 100 or more from one surface to another, the activation energies are all nearly the same.

### Multilayer Adsorption

At temperatures below 150°C, the decomposition rate was found to increase with a decrease in temperature, contrary to the usual expectation. The effect of temperature at a fixed value of the  $H_2O_2$  partial pressure is shown on Figure 27, and Figure 28 shows the effect of  $H_2O_2$  partial pressure at each of two temperatures studied, 110° and 120°C.

This effect is presumably caused by a very large increase in the amount of hydrogen peroxide adsorbed as the temperature is lowered in this range. As a guide, Figure 28 shows the partial pressure of  $H_2O_2$  that would exist in equilibrium above a liquid containing  $H_2O_2$  and  $H_2O$  at 110°C., and also at 120°C. The data at the higher partial pressure of  $H_2O_2$  are scattered; indeed the runs made at 110°C. and partial pressures of 0.08 to 0.09  $H_2O_2$  are in the range for condensation to occur. However, the data at the lower  $H_2O_2$  partial pressures, as compared on Figure 27, are unequivocal.

The adsorption of vapor from  $H_2O_2-H_2O$  vapor mixtures onto glass surfaces has been reported by Giguere (10), Baker and Ouellet (2), Mackenzie and Ritchie (17), and Tamres and Frost (33) and various tests have indicated that at least a portion of the vapor adsorbed was hydrogen peroxide. Some adsorption has been noted at temperatures as high as  $175^\circ C$ . (10), although, of course, the amount adsorbed would increase as a function of the ratio of total pressure to saturation pressure. For example, recent studies on adsorption of water vapor on glass at  $30^\circ C$ . showed that the thickness of the adsorbed layer ranged from  $620\text{\AA}$  at  $P/P_0$  of 0.9976 to  $37\text{\AA}$  at  $P/P_0$  of 0.505 (9).

#### Comparison of Vapor Decomposition Rate to Liquid Decomposition Rate

The decomposition of highly purified aqueous hydrogen peroxide solutions is believed to be exclusively a surface process in laboratory-sized vessels. Since the amount of adsorption from the vapor phase increases as the temperature is lowered, to a multilayer infinitely thick as the condensation temperature is reached, one might expect to find a smooth transition from vapor-phase decomposition rates to liquid-phase decomposition rates as the temperature is lowered. For a rough comparison, consider the case of a hydrogen peroxide vapor mixture containing 0.125 atm  $H_2O_2$  and 0.875 atm.  $H_2O$  at  $120^\circ C$ ., its saturation pressure.

As a basis for comparison one may take the data reported by Roth and Shanley (26) on the rate of decomposition of very highly purified 99%  $H_2O_2$  liquid at  $100^\circ C$ . in small laboratory Pyrex flasks. They reported that their reaction was almost wholly heterogeneous. Using their temperature coefficient of 2.5 for each  $10^\circ C$ . temperature rise and estimating the surface--volume ratio of their vessels to be about  $1\text{ cm}^{-1}$ , one would predict a decomposition rate in the liquid phase of about  $2 \times 10^{-6}$  moles/(min)( $\text{cm}^2$ ) at  $120^\circ C$ . This is to be compared to  $7.5 \times 10^{-6}$  moles/(min)( $\text{cm}^2$ ) which is the approximate value extrapolated from the present studies for vapor at  $120^\circ C$ . The comparison is remarkably close considering the possible variations in activities of Pyrex surfaces and other factors, and it suggests that there is no abrupt transition in the decomposition mechanism as one goes from the liquid to the vapor phase. Very highly purified liquid  $H_2O_2$  samples in laboratory vessels show a decomposition rate which is independent of concentration (i.e. zero order) so that this factor does not enter into the above analysis. Approximately the same liquid phase rate would be calculated from the data reported by Schumb (30) on very pure samples but of slightly lower concentrations.

Roth and Shanley reported that in their studies at  $30^\circ C$ , a portion of the decomposition seemed to be occurring heterogeneously in the vapor phase, based on the effects noted on changing the ratio of immersed vessel surface to liquid volume by varying the

liquid content of a particular flask. The rate of decomposition on immersed surface was estimated by them to be about 3 times as great per unit area as that on surface exposed to the vapor.

Their observation and the above results reported here both show that in the conventional stability tests carried out routinely on liquid hydrogen peroxide samples, considerable error may be introduced by neglecting the possibility of heterogeneous vapor-phase decomposition. The error would of course be greater the greater the fraction of the surface exposed to vapor, but would presumably also increase with increase in  $H_2O_2$  concentration and with temperature, both of which would increase the partial pressure of  $H_2O_2$  in the vapor phase.

### Polymers and Plastics

Because of the thermal properties of these organic substances, some were studied at 215°C while others were studied at 120°C.

#### High Temperature Polymers

Fluorolube A Pyrex tube was coated with Fluorolube GR grease, an addition polymer of trifluorovinyl chloride. The rate of decomposition at 215°C. is shown in Figure 29. (condition A). The activity of this surface was about half that of silica when the hydrogen peroxide partial pressure was 0.04 atm. This polymer is stable to approximately 300°C. but it melts in the vicinity of 100°C. In view of this low melting point, the permanency of this coating was tested by passing live steam for several hours over the outside of the vertical sealed tube. The activity of this tube, designated as condition B, was again determined. As is seen on Figure 29, the rate of decomposition increased indicating that the Fluorolube no longer coated the Pyrex tube. Another indication was the fact that although water will not wet a Fluorolube surface, it did wet Tube 21 in Condition B.

Teflon The decomposition on Teflon, a polymer of tetrafluoroethylene, was investigated at both 215°C and 120°C. The surface studied at 215°C was a rod placed coaxially in a Pyrex tube, tube 25 (in condition B); at 120°C it was a Teflon strip placed in a Pyrex tube, tube 25 (in condition D). The width of the strip was the same as the diameter of the tube. These results (Figures 30 and 32) show that the rate of decomposition of Teflon is about 10 times higher than on Pyrex at 215°C, but only about twice as high at 120°C. The small difference at 120°C probably is a result of the fact that multilayer adsorption occurs on glass, as discussed previously, whereas Teflon, which is not wetted by water, presumably would have low adsorptivity for  $H_2O_2$ .

Methyl Trichloro Silane Methyl trichloro silane bonds chemically to glass to form a stable coating which is not wetted by water. The rate of hydrogen peroxide vapor decomposition was measured on this surface, tube 28, and the results are given on Figure 31. The silane coating was apparently not attacked by the hydrogen peroxide vapor; the activity of the surface was slightly less than that of the untreated surface.

### Low Temperature Polymers

Methyl methacrylate is one of the few polymers which will form a continuous stable film on glass (11). However, a film of this substance on a Pyrex tube was attacked by the hydrogen peroxide and was blistered and bleached. A strip of polyethylene placed in a Pyrex tube became very soft and was attacked badly by the hydrogen peroxide vapor. A strip of Koroseal, a polymer of vinyl chloride, placed in a Pyrex tube, show slight bleaching by  $H_2O_2$  vapor.

The activities of several polymers at  $120^\circ C$  are shown in Figure 32.

Summary In the first column of Table V are summarized the rates of decomposition on the various polymeric surfaces when the hydrogen peroxide partial pressure was 0.04 atm. In the second column of Table V are tabulated the rates of decomposition of 90% hydrogen peroxide liquid on some of these surfaces at  $66^\circ C$  (3). There is seen to be a positive correlation between the catalytic activity of a surface for the rate of decomposition of hydrogen peroxide liquid and for the vapor. The polyethylene value was high for the decomposition of the vapor because at  $120^\circ C$  the plastic was in an almost molten state.

Teflon is the most satisfactory polymer for use with hydrogen peroxide vapor at moderately elevated temperatures since it is unattacked. However, because of the high cost of this material it may be more satisfactory to use Koroseal for short term usage. Fluorolube grease would be an inert stopcock grease and might in addition be used to coat metallic surfaces. Methyl trichloro silane and Fluorolube coatings, which are not wetted by water, might very substantially decrease the rate of decomposition of  $H_2O_2$  vapor on Pyrex or other glass surfaces at temperatures near saturation where multi-layer adsorption is the important factor in causing increased decomposition rates.

Table V

## RATES OF DECOMPOSITION ON POLYMERS

Surface	Rate of Decomposition of H <sub>2</sub> O <sub>2</sub> vapor x 10 <sup>6</sup> (moles/min cm <sup>2</sup> ) P <sub>H<sub>2</sub>O<sub>2</sub></sub> = 0.04 atm.	Percentage of 90% H <sub>2</sub> O <sub>2</sub> liquid decomposed/week at 66°C.
T = 120°C		
Pyrex	2	---
Teflon	5	2.6
Koroseal	14	18-29
Methyl methacrylate	5 (attacked)	---
Polyethylene	30 (attacked)	1.7
T = 215°C		
Pyrex, acid rinsed	about 2	---
Fluorolube GR grease	1	1.7
Teflon	24	2.6
Methyl Trichloro Silane on Pyrex	1	---

Metals

Only metals to which hydrogen peroxide is relatively inert were studied: stainless steels types 303, 304, and 416, 2S aluminum, tin and tantalum. In each case, a rod of the metal about 0.23 cm in diameter and 16-17 cm. long was placed coaxially in a Pyrex tube. The rate data reported were calculated from the difference between the rates of decomposition with and without the rod present, calculated per unit area of metal rod.

Stainless Steels

Electrolytically Polished The rates of decomposition of hydrogen peroxide vapor at 150°C on polished stainless steels 304, 303, and 416 are given on Figures 33, 34, and 35 respectively. The electrolytic polishing procedure, which is described by Uhlig (34), causes preferable anodic solution of high points on the surface of the metal so that eventually the surface is levelled to a microscopic plane.

On these electrolytically polished steels there was no observable effect of aging during the decomposition studies at 150°C. The elapsed time between runs 287 and 289 on Figure 33 was two hours;

the time between runs 273 and 298 on Figure 34 was six hours; and on Figure 35, the time between runs was only one hour. Prior to these determinations at 150°C, these surfaces had been studied at 120°C, which may have caused an initial aging. The catalytic activity of the surface of stainless steel 416 increased steadily with time during runs at 120°C, but the others were affected only slightly. It has been reported that all of the stainless steels are bronzed by 90% hydrogen peroxide liquids (3), although stainless steels types 303 and 304 are reported to have greater chemical resistance than type 416 because they contain nickel. Types 303 and 304 are nearly the same with the exception that type 303 is softer because traces of selenium are present.

**Pickled and Passivated Surfaces** The rates of decomposition of hydrogen peroxide vapor on pickled and passivated stainless steels 303 and 304 are presented on Figures 36 and 37. By comparison with Figure 34, it can be seen that these treatments greatly lowered the catalytic activities of these surfaces.

In the pickling operation the steel was immersed in a 15-20% by weight sulfuric acid solution with no inhibitor, for 45 minutes at 150-160°F. The sample was then immersed in a 8-10% by volume nitric acid solution containing 1 1/4 to 2% by volume hydrofluoric acid at 140-160°F. (27). With no inhibitor present, the pickling solution preferentially dissolves FeO and Fe, leaving a surface containing mainly Cr<sub>2</sub>O<sub>3</sub> and NiO, with small amounts of Fe<sub>2</sub>O<sub>3</sub> (7a,16a,32a).

In the passivation operation, the sample is first pickled and then treated with a 20-40% nitric acid solution for 30 minutes at 120-170°F. (27). The purpose of this treatment is to form a resistant oxidized film on the metal. Examination of Figure 37 indicated that the oxide film formed by nitric acid is no less reactive than that formed by hydrogen peroxide on a pickled surface.

### Aluminum

**Electropolished** The activity of a electropolished aluminum sample is shown on Figure 38. The elapsed time between runs 304 and 305 was one hour; there was no evidence of aging during these studies. Aluminum is not chemically attacked by 90% hydrogen peroxide solutions (3).

After completion of an electropolishing process the metal reacts with the electrolyte which was a solution of sulfuric and phosphoric acids. The final surface therefore probably consisted of a mixture of oxides and phosphates.

**Anodized** A hard stable oxide coating is formed on aluminum by anodizing the sample (22). The rate of hydrogen peroxide decomposition can be seen on Figure 39.

Pickled An oxide film can also be formed on aluminum by pickling the sample in a solution containing 6 oz. of sodium hydroxide per gallon of water at 180°-200°C. Then the rod is immediately immersed for a few seconds in a solution containing one part HNO<sub>3</sub> and one part H<sub>2</sub>O (21). The density of this film is probably different from that of an anodized surface. The rate of decomposition on this surface is shown on Figure 40.

Phosphated A phosphate film can be formed on aluminum by treating it with a phosphoric acid solution (18). The activity of this surface is shown on Figure 39.

### Tin

The tin used in this work was essentially pure. The rates of decomposition of hydrogen peroxide vapor were determined on two samples, one of which was rinsed in carbon tetrachloride and water to remove the grease, and the other which was dipped in a 20% nitric acid solution for a split second. The rates of decomposition are on Figure 41. The acid attacked the tin violently and formed a visible oxide coating.

Tin is not attacked by 90% hydrogen peroxide liquid but it has the disadvantage as a material of construction in that it changes allotropic forms with changes in temperature (23).

### Tantalum

The rates of hydrogen peroxide vapor decomposition at 150°C were determined on two samples of pure tantalum. One piece was degreased with carbon tetrachloride and water, while the other was treated with a 40% nitric acid solution for 30 minutes at 120°F. The results on Figure 42 indicate that the rates were equal on each.

The effect of aging of tantalum was not studied, but it might be expected to be slight since tantalum is one of the more inert metals to oxidation.

### Summary

In the first column of Table VI are summarized the rates of decomposition at 150°C of hydrogen peroxide vapor on metallic surfaces when the partial pressure of hydrogen peroxide was 0.03 atm.

TABLE VI  
DECOMPOSITION RATES ON METALLIC SURFACE AT 150°C

	<u>Vapor</u> Rate of decomp. x 10 <sup>6</sup> (moles/min cm <sup>2</sup> ) (P H <sub>2</sub> O <sub>2</sub> = 0.03 atm.)	<u>Liquid</u> Percent of 90% H <sub>2</sub> O <sub>2</sub> Decomposed/week 66°C
Stainless Steels		
303 Electropolished	40	50-60 (nitric Acid)
Pickled and Passivated	17	
304 Electropolished	125	
Pickled	20	
Pickled and Passivated	20	
416 Electropolished	115	
2S Aluminum		
Electropolished	110	
Phosphated	105	
Anodized	45	3
Pickled	35	
Tantalum		
Degreased	42	
Acid treated (nitric)	42	
Tin		
Degreased	45	6.4-28.7
Acid treated (nitric)	31	

In the second column of Table VI are the percentages of 90% hydrogen peroxide liquid which are decomposed per week at 66°C (3).

It is observed that pickled stainless steels types 303 and 304 and pickled aluminum surfaces have the most desirable properties for use with hydrogen peroxide vapor. It is possible, however, that with time, the stainless steel surfaces may age.

Other salient observations from this table are: (1) stainless steels becomes less reactive as the iron is preferentially removed from the surface; (2) oxide coatings on aluminum are less reactive than phosphated coatings; and (3) tantalum and tin surfaces are nearly as inert as the pickled stainless steel and aluminum surfaces. However, they are much more expensive than the latter materials.

Although the data available for comparative purposes are sparse, there is a general qualitative correlation between the activities for the decomposition of the liquid and vapor on these metallic surfaces.

Various metallic surfaces were studied at 120°C; however, these data scattered widely because of the masking effect of the

decomposition on Pyrex, which at 120°C varies greatly with slight temperature changes, presumably because of multilayer absorption effects.

### Reaction Mechanism

#### Derivation of Rate Equation

In three reactors (two consisting of boric oxide surfaces on Pyrex, the third a pickled 2S aluminum surface), a sufficiently wide range of conditions was studied that the heterogeneous decomposition rates could be expressed mathematically as a function of temperature and composition. If the Langmuir adsorption model is assumed, i.e. that the reactants are adsorbed in a monolayer on various active sites on the catalytic surface from whence the reaction proceeds, equations can be derived for various reaction mechanisms with each of several rate-controlling steps. The following mechanisms were considered: (1) reaction between two adsorbed hydrogen peroxide molecules; (2) reaction between one adsorbed molecule of hydrogen peroxide and a molecule in the vapor phase; (3) reaction between adsorbed OH radicals, resulting from the dissociation of a hydrogen peroxide molecule, and a molecularly adsorbed hydrogen peroxide molecule; (4) reaction between adsorbed OH radicals and a hydrogen peroxide molecule in the vapor phase; and (5) uncatalysed reaction in the vapor phase. For each mechanism the following rate-controlling steps were considered: (1) rate of surface reaction controlling, (2) rate of adsorption of molecular hydrogen peroxide controlling, (3) rate of adsorption of OH radicals controlling; and (4) rate of desorption of water controlling. These various combinations provided fifteen different possible mathematical relationships (the same form may result from more than one postulated mechanism and rate-controlling step.)

The experimental results for the decomposition on the three surfaces all fitted an equation of the form:

$$-\frac{dn_{\text{H}_2\text{O}_2}}{A d\theta} = \frac{\alpha K_{\text{H}_2\text{O}_2} P_{\text{H}_2\text{O}_2}^2}{(1 + \sqrt{K_{\text{H}_2\text{O}_2} P_{\text{H}_2\text{O}_2}} + K_{\text{H}_2\text{O}} P_{\text{H}_2\text{O}})^2} \quad (1)$$

Of the fifteen derived relationships, only three acceptably fitted the data; equation (1) was arbitrarily chosen. The other two acceptable forms were with the bracketed term in the denominator raised to the first or third power instead of the second.

For a Pyrex tube coated with boric oxide with a surface-to-volume ratio of 1.75 cm<sup>-1</sup>, tube 9 in conditions A, B, and D, the experimental data and the theoretical curves for the three temperatures studied can be seen on Figures 43, 44, and 45. The temperature dependent terms for equation (1) are:

$$K_{\text{H}_2\text{O}_2} = 7.34 \times 10^7 e^{-11.3 \times 10^3 / RT}$$

$$K_{\text{H}_2\text{O}} = 3.82 \times 10^{-3} e^{7.76 \times 10^3 / RT}$$

$$\alpha K_{\text{H}_2\text{O}_2} = 1.1$$

The average deviations of the experimental data from the theoretical values are 7% at 180°C; 16% at 215°C; and 9% at 250°C.

In another boric oxide surface, tube 9 plus rods, with a surface to volume ratio of  $5.6 \text{ cm}^{-1}$ , the temperature dependent terms are:

$$K_{\text{H}_2\text{O}_2} = 9.18 \times 10^5 e^{-6.36 \times 10^3 / RT}$$

$$K_{\text{H}_2\text{O}} = 3.15 \times 10^{-6} e^{13.97 \times 10^3 / RT}$$

$$\alpha K_{\text{H}_2\text{O}_2} = 1.05$$

The experimental data and theoretical curves are plotted on Figures 46, 47, and 48.

For the third surface, a pickled 2S aluminum surface, the experimental data and curves are on Figures 40 and 49. The terms for equation (1) were found to be:

$$K_{\text{H}_2\text{O}_2} = 2.72 \times 10^{-9} e^{7.4 \times 10^3 / RT}$$

$$K_{\text{H}_2\text{O}} = 1.12 \times 10^{-11} e^{20.9 \times 10^3 / RT}$$

$$\alpha K_{\text{H}_2\text{O}_2} = 0.111$$

Because of diffusional effects, there will be a slight difference between the interfacial partial pressures and the bulk partial pressures, which would be greater at the higher rates of reaction. This inaccuracy does not alter the general form of the equations, but would slightly affect the values of the temperature-dependent terms.

### Reaction Mechanisms

The mechanisms corresponding to the three acceptable equations are:

1. Reaction of adsorbed OH radicals and molecularly adsorbed hydrogen peroxide
  - a) Desorption of water controlling (denominator of equation (1) raised to first power)
  - b) Surface reaction controlling (denominator of equation (1) raised to third power)
2. Reaction of adsorbed OH radicals and hydrogen peroxide in the gas phase with the rate of surface reaction controlling (equation (1)).

In all three cases a hydrogen peroxide molecule is visualized as being adsorbed on two adjacent sites and dissociating to form two adsorbed OH radicals. One of these radicals then reacts with a hydrogen peroxide molecule, either adsorbed or in the vapor phase, to form water and an OOH radical. The OOH radical then combines with the adjacent OH radical, perhaps with the aid of a third body, to form water and oxygen which are then desorbed to leave the original two adjacent unoccupied active sites. Since it has been hypothesized in this work that the active sites for decomposition are electron donor sites, it is possible that the OH and OOH exist as ions rather than radicals.

This reaction mechanism is also consistent with a first order reaction, which has been reported under different experimental conditions by other investigators (2,10). If the OOH radical were to react with another hydrogen peroxide molecule to form as products water, oxygen and an adsorbed OH radical, instead of reacting with an adjacent OH radical as proposed above, then the model would be a surface on which all active sites are occupied with either an OH radical or an OOH radical. The reaction rate would be proportional to the concentration of hydrogen peroxide molecules which react with these adsorbed radicals, which describes a first order reaction.

The model system considered here is quite possibly an oversimplification of the true nature of the processes occurring on catalytic surfaces, and therefore one must be somewhat skeptical of the conclusions as to the mechanism involved when they are based on a matching of the mathematical form of the rate equation found against those derived from various models. Yet the steps of this heterogeneous mechanism are consistent with the steps proposed for the homogeneous decomposition of the vapor (28) and for the reaction steps proposed for both the homogeneous and heterogeneous catalytic decomposition of the liquid (1). In studies of the heterogeneous decomposition of hydrogen peroxide liquid on

supported manganese oxide catalysts, Hool and Selwood (13, 14) found that a minimum of two adjacent manganese ions is a necessary condition for the decomposition.

### Homogeneous Decomposition

The homogeneous decomposition does not become appreciable until relatively high temperatures are reached and experimental problems then are quite difficult. The data collected under these conditions were not extensive, but they do provide some information concerning the magnitude and characteristics of the homogeneous reaction.

### Variation of Surface to Volume Ratios

The surface to volume ratio of a boric oxide coated Pyrex tube, tube 9, was increased from  $1.75 \text{ cm}^{-2}$  to  $5.6 \text{ cm}^{-2}$  to determine if the homogeneous decomposition were appreciable in the temperature range from  $180\text{--}250^\circ\text{C}$ . This change was made by adding to the tube a bundle of boric oxide coated Pyrex rods which uniformly filled a cross section of the tube. A comparison of the rate of decomposition at  $180^\circ\text{C}$  can be made by comparing Figures 43 and 46; at  $215^\circ\text{C}$ , Figures 44 and 47; and at  $250^\circ\text{C}$ , Figures 45 and 48. The fact that the rate per unit area of surface is independent of the surface to volume ratio, within the accuracies of reproducing surface, shows that homogeneous reaction can not be detected at these temperatures.

### High Temperature Studies

The rate of decomposition of hydrogen peroxide vapor in the temperature range from  $215^\circ\text{C}$  to  $490^\circ\text{C}$  was investigated in three Pyrex tubes, each of which previously had been treated with 4N phosphoric acid and each of which had a surface area of  $590 \text{ cm}^2$  and a volume of  $300 \text{ cm}^3$ . The results are shown on Figure 50.

Two facts show quite clearly that a transition from heterogeneous to homogeneous decomposition occurred in the temperature range of  $400$  to  $450^\circ\text{C}$ ; (1) the sharp increase in decomposition rate with temperature and (2) the fact that different tubes showed different decomposition rates in the lower (heterogeneous) temperature region but the same results in the higher temperature region. The data in the heterogeneous range were obtained at  $\text{H}_2\text{O}_2$  partial pressures of  $0.025$  to  $0.038$  atmosphere, those in the homogeneous range from  $0.006$  to  $0.029$  atmospheres. To put the results on a comparable basis, the rates of decomposition were recalculated for a  $\text{H}_2\text{O}_2$  partial pressure of  $0.02$  atmosphere, assuming that in the homogeneous range the rate is proportional to the  $3/2$  power of the  $\text{H}_2\text{O}_2$  concentration, and in the heterogeneous range that the concentration effect is the same as that found at lower temperatures.

Analysis of the data in the homogeneous range is made difficult by two factors: (1) the rate is so rapid under these conditions that a large fraction of the  $H_2O_2$  entering the reactor decomposed therein, so that for data analysis it must be treated as an "integral reactor", (2) the temperatures reported are an average of the bath temperature and that of the vapor entering the reactor. This is a satisfactory measure of reaction temperature when reaction takes place exclusively on the tube wall. However in the homogeneous range the exothermicity of the reaction may cause the vapor to be appreciably hotter than the tube walls. To estimate this factor, the temperature variation of the vapor as a function of tube length was calculated for various inlet  $H_2O_2$  concentrations, assuming the heat transfer coefficient to be  $3.5 \text{ BTU}/(\text{hr.})(^\circ\text{F.})(\text{ft.}^2)$ , the latter being based on the Reynolds number, with allowance for entering turbulence. It was concluded that for only one set of runs (Runs 270A, B & C, at  $460^\circ\text{C}$  and  $P_{av} = 0.029$ ) was this factor an appreciable source of error and that here the vapor temperature was about  $10^\circ\text{C}$ . higher than the wall temperature. For plotting on Fig. 51, (discussed below) the observed values were therefore corrected using the Arrhenius equation with an activation energy of 55 kcal.

To analyze data from an integral reactor requires knowledge of the order of the reaction to determine the correct manner in which to average inlet and exit  $H_2O_2$  concentrations. Therefore, it is necessary to assume a reaction order in order to analyze the data, after which the assumption may be checked by examining a set of data obtained at one temperature. Assuming the reaction rate to be proportional to the  $3/2$  power of the  $H_2O_2$  partial pressure,

$$-\frac{dn_{H_2O_2}}{Vd\theta} = k P_{H_2O_2}^{3/2} \quad (2)$$

where the average value of  $P_{H_2O_2}$  is given by:

$$P_{H_2O_2} = \left[ \frac{P_{in}^{1/2} P_{out}^{1/2} + P_{out}^{1/2} P_{in}^{1/2}}{2} \right] \quad (3)$$

the homogeneous rate data obtained at somewhat differing average partial pressures may be recalculated to a common basis of a  $H_2O_2$  partial pressure of 0.02, yielding the curve in Figure 50 for the homogeneous reaction. The slope of this curve correspond to an activation energy of about 55 kcal/gm.mole.

To check the assumption of a 3/2 order reaction, data obtained at 460°C. and several concentrations were plotted as on Figure 51. The slope corresponds to a 3/2 order reaction. Further evidence for a 3/2 order reaction comes from the data of Miss Huang (15) which were obtained in the same type of apparatus, differing principally in that the reaction temperature was determined from 5 thermocouple wells placed equidistantly along the reaction tube. A group of 9 runs at temperatures between 466°C and 489°C. and at mean H<sub>2</sub>O<sub>2</sub> partial pressures of from 0.001 to 0.035 atmosphere were available for evaluation. The rate data were converted to the common basis of 475°C. using the Arrhenius equation and an activation energy of 55,000 kcal. Although the data scatter somewhat, the results, shown on Figure 52, clearly correspond to a 3/2 order expression rather than a first or a second order. The data of Miss Huang when recalculated to 475°C and 0.02 partial pressure of H<sub>2</sub>O<sub>2</sub> and allowing for the difference in reactor volumes. correspond to a rate of homogeneous reaction about 30% less than that shown in Figure 50.

Only one other study of the homogeneous reaction that is more than fragmentary has been reported. McLane (19) obtained data at average concentrations of 0.002 atmosphere pressure of H<sub>2</sub>O<sub>2</sub> and below at temperatures of 470-540°C in boric acid-coated Pyrex. His rate reportedly followed a first-order expression and in the lowest surface-volume ratio vessel studied, (S/V = 3 cm<sup>-1</sup>) he reported an activation energy of 50,000 calories.

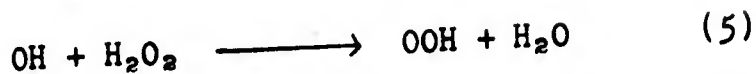
There are several important differences between his experimental conditions and those in the present study. The H<sub>2</sub>O<sub>2</sub> concentrations here were one to two orders of magnitude greater; the surface-volume ratio of the present vessel was about 2 cm<sup>-1</sup>, compared to 3 cm<sup>-1</sup> of McLane, and the flow pattern here approximated slug flow whereas that of McLane appeared to be close to that of a completely mixed reactor. The present rate data are about twice those reported by McLane if the rate is taken to be proportional to the 3/2 power, or about ten times those of McLane if the reaction were assumed to follow a first order expression. This most probably reflects an increase in chain length of the reaction as the surface-volume ratio is lowered and the H<sub>2</sub>O<sub>2</sub> concentration is raised.

The most probable initiating step in the reaction is

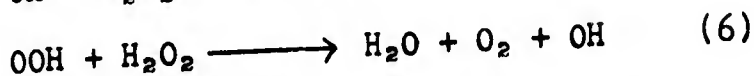


The energy required for this reaction is about 53 kcal/g.mole whereas about 90 kcal/g.mole would be needed for the only alternate initiating step, formation of H and OOH.

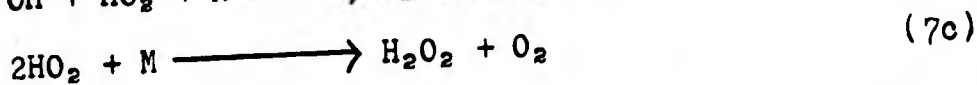
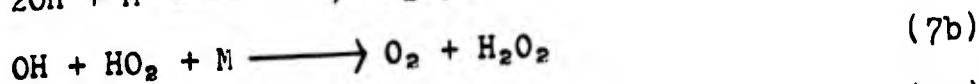
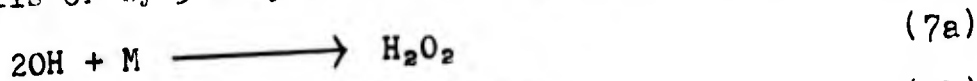
Chain propagation is most probably by



and



both of which are exothermic whereas all chain branching steps are endothermic. Chain breaking can occur by absorption of radicals on the walls or by 3-body combination reactions of OH or OOH, thus



If the rates of reactions 4, 5, 6 and (7a) are formulated in terms of the appropriate rate constants and reactant concentrations, and the rate of production and destruction of each of the free radicals is equated, one can derive the following expression:

$$-\frac{dn_{\text{H}_2\text{O}_2}}{Vdt} = 2k_6 \sqrt{\frac{2k_4}{k_7}} \left(\frac{1}{RT}\right)^{3/2} P_{\text{H}_2\text{O}_2} \quad (8)$$

A 3/2 order expression is also obtained if one of the other free radical combination reactions is chosen instead of (7a). However, if 3 body free radical combination reactions are regarded as negligible and chain stopping is assumed to occur by adsorption on walls, the mathematical formulation leads instead to a second order expression. The fact that the decomposition rate in fact followed a 3/2-order expression suggests that the 3 body free radical recombinations were the chain stopping mechanism here and not wall reactions.

The existence of long chains here is indicated by a comparison of the observed decomposition rate with the number of collisions of hydrogen peroxide molecules in which the energy is greater than 55,000 calories/g.mole.

The measured decomposition rate at 460°C. and  $\text{H}_2\text{O}_2$  partial pressure of 0.02 atmospheres corresponds to about  $1.8 \times 10^{17}$  molecules decomposing per cc per min. Assuming that the fraction of collisions having activation energies greater than 55,000 equals  $e^{-E/RT}$ , the number of such collisions is about  $1.1 \times 10^{12}$  per  $\text{cm}^3$  per sec. Even allowing for the possibility that the activation energy may be shared between more than 2 "squared terms" and therefore that the fraction of effective collisions may be somewhat greater than

$e^{-E/RT}$ , it appears that long chains are involved here, perhaps of the order of magnitude of  $10^6$ .

LITERATURE CITATIONS

- (1) "Advances in Catalysis" Vol. IV, Academic Press, New York, N. Y., 1952.
- (2) Baker, B. E., and Ouellet, C., Can. J. Research, 23B, 167 (1945).
- (3) Buffalo Electrochemical Company, "Engineering Materials for Use with 90% Hydrogen Peroxide," Buffalo New York, 1950.
- (4) Cook, G. A., U. S. Patents 2,368,640 and 2,368,806, Feb. 6, 1945.
- (5) Coward, J. N. and Turner, W. E. S., J. Soc. Glass Tech., T22, 309 (1938)
- (6) Douglas, R. W., and Isard, J. O., J. Soc. Glass Tech., 33, 289 (1949).
- (7) Dowden, D. A., J. Chem. Soc. (London), I, 242 (1950).
- (7a) Evans, U. R., "Metallic Corrosion, Passivity and Protection", E. Arnold & Co., London, England, 1946.
- (8) Fitzgerald, J. V., Glass Ind., 30, 259 (1947).
- (9) Garbatski, U. and Folman, M., J. Chem. Phys, 22, 2086 (1954).
- (10) Giguere, P. A., Can. J. Research, 25B, 135 (1947).
- (11) Hedvall, J. A., Jagitsch, R., and Olsen, G., Zeits. f. Phys. Chem., 196, 23 (1950).
- (12) Hensley, J. W., Long, A. O., and Willard, J. E., Ind. Eng. Chem., 41, 1415 (1949).
- (13) Hooi, J. and Selwood, P. W., J. Am. Chem. Soc., 72, 4333 (1950).
- (14) Hooi, J. and Selwood, P. W., J. Am. Chem. Soc., 74, 1750 (1952).
- (15) Huang, Y. M., S. M. Thesis in Chemical Engineering, M.I.T., 1955.
- (16) Kondrat'eva, E., and Kondrat'ev, V. N., J. Phys. Chem. (USSR), 19, 178 (1945).
- (16a) Kubraschewski, O., and Hopkins, B. E., "Oxidation of Metals and Alloys", Academic Press, Inc., New York, 1953.
- (17) MacKenzie, R. C., and Ritchie, M., Proc. Roy. Soc., (London), A185, 207 (1946).
- (18) Manual 43, Materials and Methods, 28, 83 (1948).
- (19) McLane, C. K., J. Chem. Phys., 17, 379 (1949).

- (20) Metal Finishing, 18th Annual Ed., Guidebook, 182 (1949).
- (21) Ibid, 200 (1949).
- (22) Metal Finishing, 20th Annual Ed., Guidebook, 428 (1951).
- (23) Mellor, J. W., "A Comprehensive Treatise on Inorganic and Theoretical Chemistry", Vol. VII, Longmoors, Green and Co., London, England, 1940.
- (24) Morey, G. W., "Properties of Glass," ACS No. 77, Reinhold Publishing Co., New York, 1938.
- (25) Rees, A. L. G., "Chemistry of the Defect Solid State", London Methuen, Wiley & Co., New York, 1954.
- (26) Roth, E. M. and Shanley, E. S., Ind. Eng. Chem., 45, 2343 (1953)
- (27) Rustless Iron and Steel Corp., "Heat Treatment of Stainless Steels", Baltimore, Md., 1944.
- (28) Satterfield, C. N. Kavanagh, G. M., and Resnick, H., Ind. Eng. Chem., 43, 2507 (1951)
- (29) Satterfield, C. N., Ceccotti, P. J., and Feldbrugge, A. H. B., Ind. Eng. Chem., 47, 1040 (1955)
- (30) Schumb, W. C., Satterfield, C. N., and Wentworth, R. L., "Hydrogen Peroxide", A. C. S. Monograph No. 128, Reinhold Publishing Corp., 1955.
- (31) Selwood, P. W., in "Catalysis" Vol. I, edited by P. H. Emmett, Reinhold Publishing Corp., New York, 1954.
- (32) Sherwood, T. K. and Pigford, R. L., "Absorption and Extraction" McGraw-Hill Book Co., Inc., New York, 1952.
- (32a) Speller, F. M., "Corrosion, Causes and Prevention", McGraw Hill, New York, 1951.
- (33) Tamres, M. and Frost, A. A., J. Am. Chem. Soc., 72, 5340 (1950).
- (34) Uhlig, H. H., Trans. Electrochemical Soc., 78, 265 (1940).
- (35) Von Greffchen, W. and Berger, E., Glas. Tech. Ber., 16, 296 (1938).
- (36) Weyl, W. A., Trans. New York Aca. Sci., II, 12, No. 8, 245 (1950).
- (37) Williams, H. S. and Weyl, W. A., Glass Ind., 26, 324 (1945).

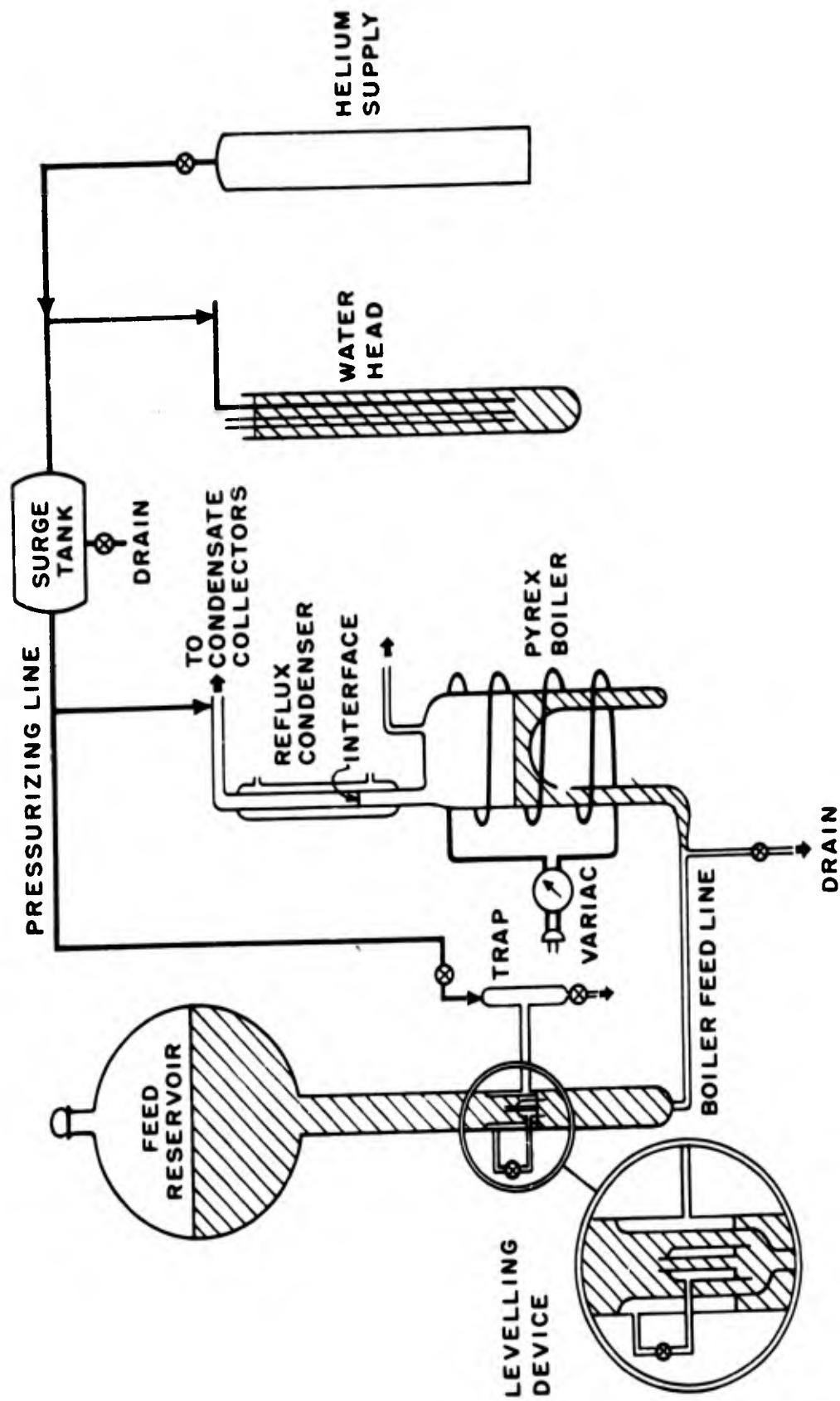


FIG.1 - HYDROGEN PEROXIDE VAPORIZATION SYSTEM

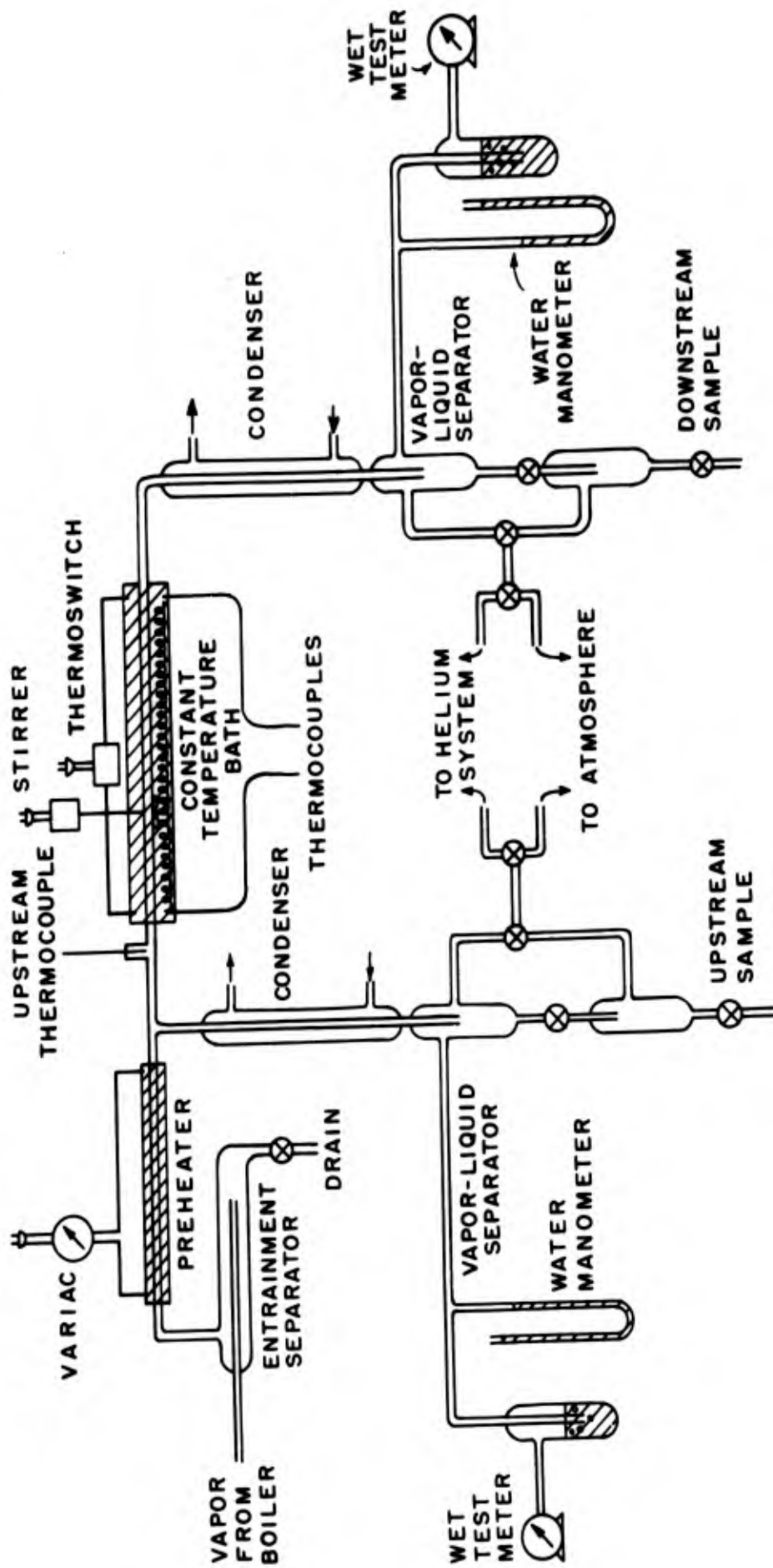


FIG. 2 - DECOMPOSITION APPARATUS (SHOWN WITHOUT INSULATION)

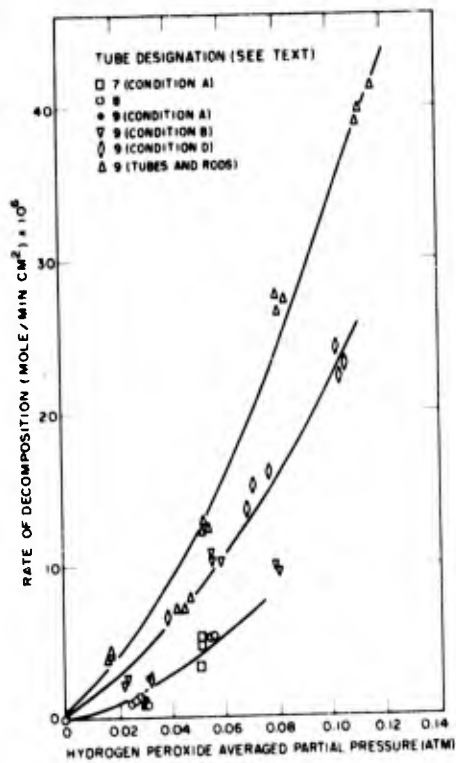


FIG 3 DECOMPOSITION RATE OF HYDROGEN PEROXIDE VAPOR ON BORIC OXIDE SURFACES (T = 215°C)

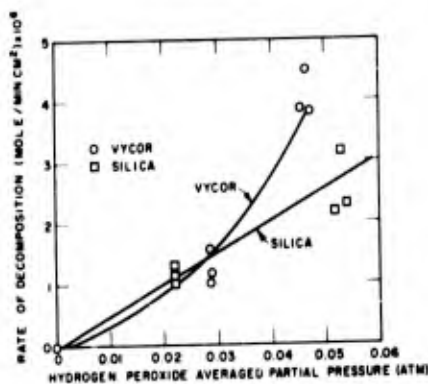


FIG 4 DECOMPOSITION RATE OF HYDROGEN PEROXIDE VAPOR ON SILICA AND VYCOR SURFACES (T = 215°C)

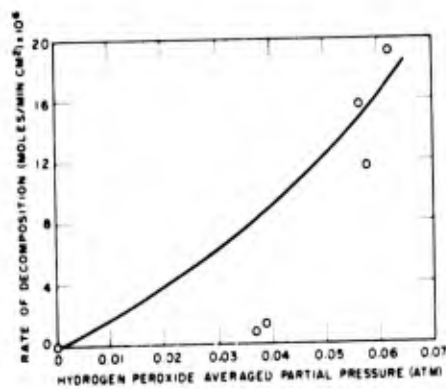


FIG 5 - DECOMPOSITION RATE OF HYDROGEN PEROXIDE VAPOR ON SOFT GLASS SURFACE (T = 215°C)

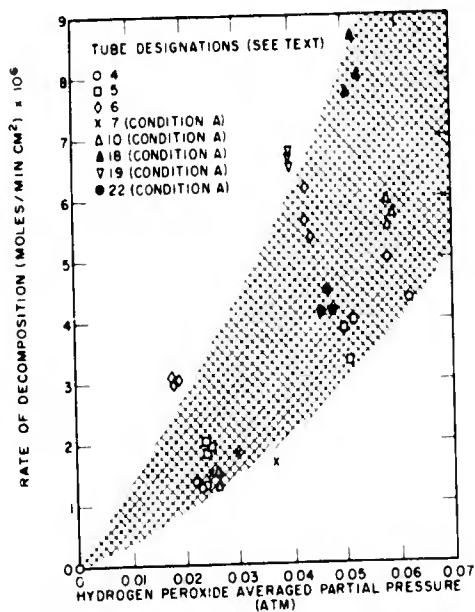


FIG 6 DECOMPOSITION RATE OF HYDROGEN PEROXIDE VAPOR ON PYREX SURFACES (T = 215°C)

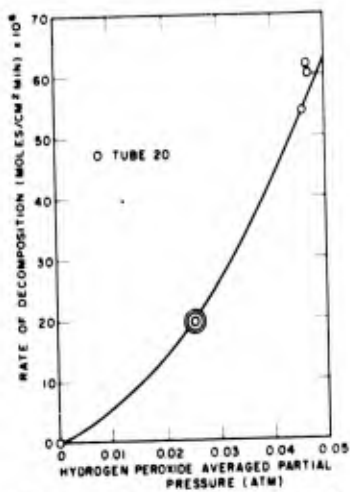


FIG 7 DECOMPOSITION RATE OF HYDROGEN PEROXIDE VAPOR ON A LEAD GLASS SURFACE (T = 215°C)

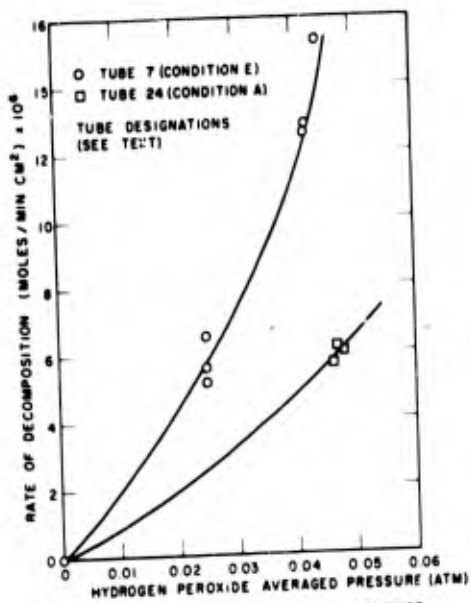


FIG 8 DECOMPOSITION RATE OF HYDROGEN PEROXIDE VAPOR ON PYREX SURFACES TREATED WITH 5% SODIUM HYDROXIDE SOLUTIONS (T=215°C)

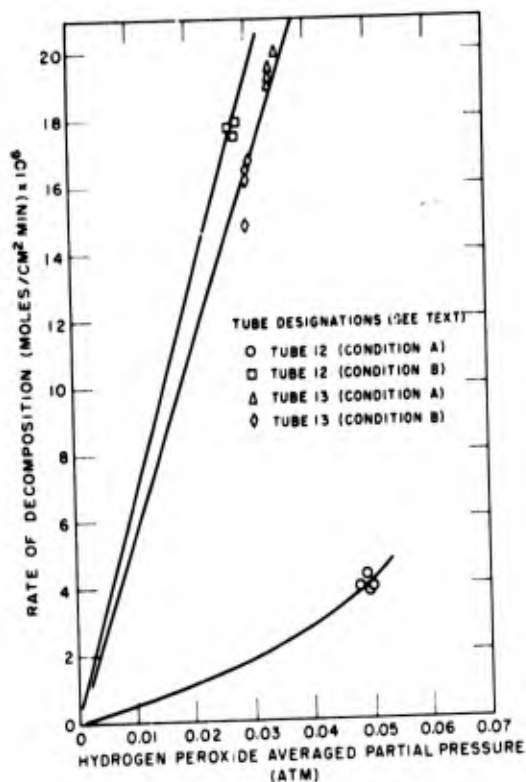


FIG 9 DECOMPOSITION RATE OF HYDROGEN PEROXIDE VAPOR ON PYREX SURFACES TREATED WITH SODIUM AND SILVER NITRATES (T=215°C)

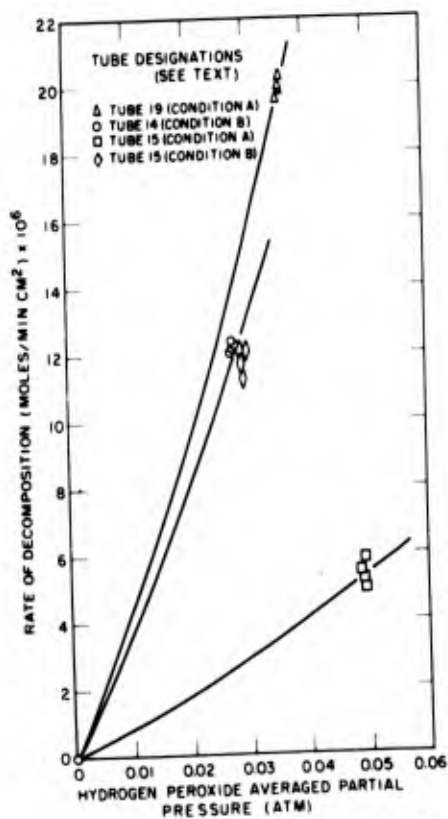


FIG 10 DECOMPOSITION RATE OF HYDROGEN PEROXIDE VAPOR ON PYREX SURFACES TREATED WITH SODIUM AND FERRIC NITRATES (T=215°C)

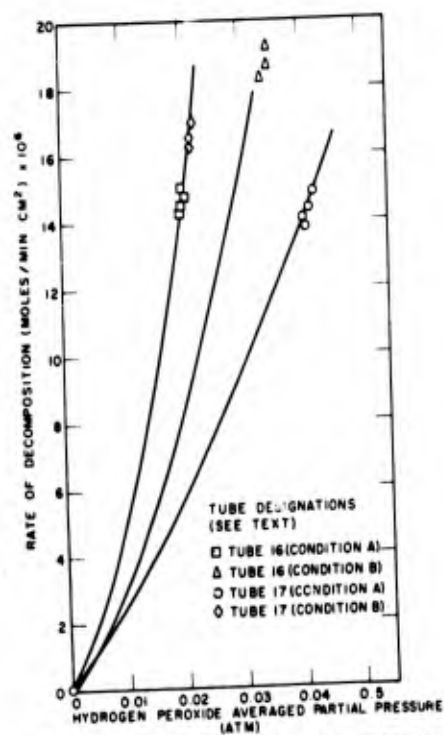


FIG 11 DECOMPOSITION RATE OF HYDROGEN PEROXIDE VAPOR ON PYREX SURFACES TREATED WITH SILVER AND FERRIC NITRATES (T=215°C)

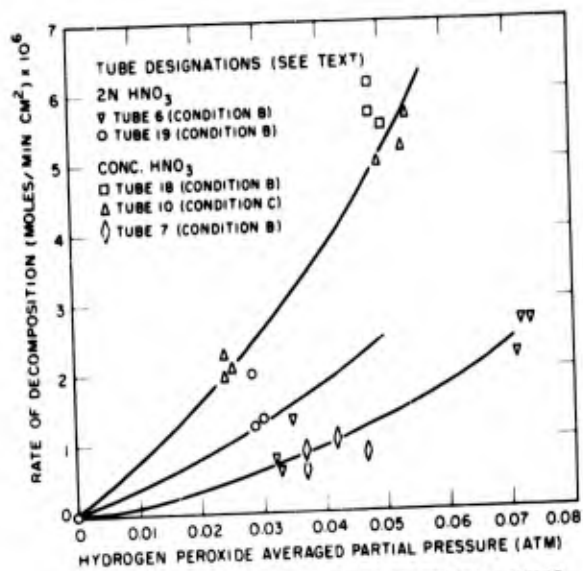


FIG 12 DECOMPOSITION RATE OF HYDROGEN PEROXIDE VAPOR ON PYREX SURFACES TREATED WITH NITRIC ACID (T=215°C)

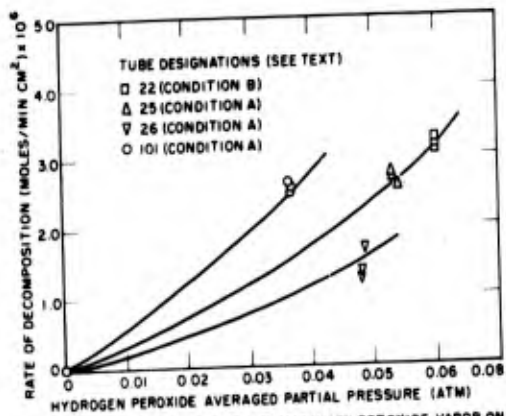


FIG 13 DECOMPOSITION RATE OF HYDROGEN PEROXIDE VAPOR ON PYREX SURFACES TREATED WITH 4N PHOSPHORIC ACID (T=215°C)

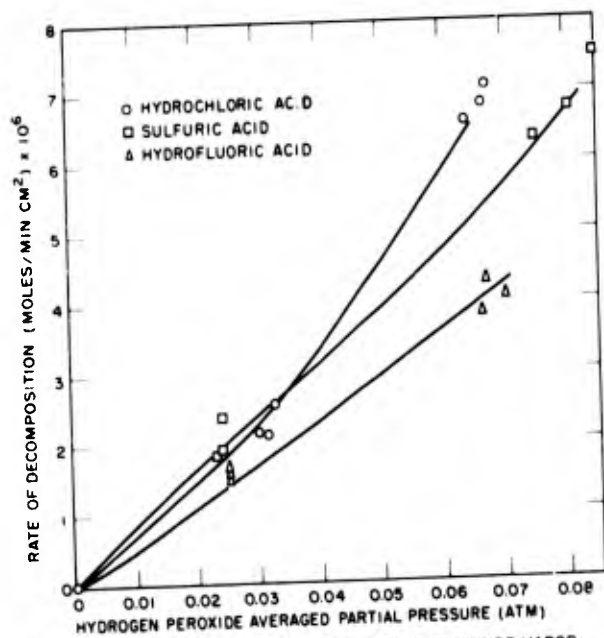


FIG 14 DECOMPOSITION RATES OF HYDROGEN PEROXIDE VAPOR ON PYREX SURFACES TREATED WITH VARIOUS ACIDS (T = 215°C)

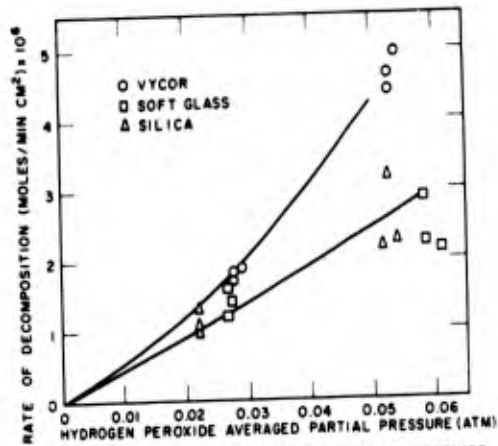


FIG 15 DECOMPOSITION RATE OF HYDROGEN PEROXIDE VAPOR ON VARIOUS ACID RINSED GLASS SURFACES (T = 215°C)

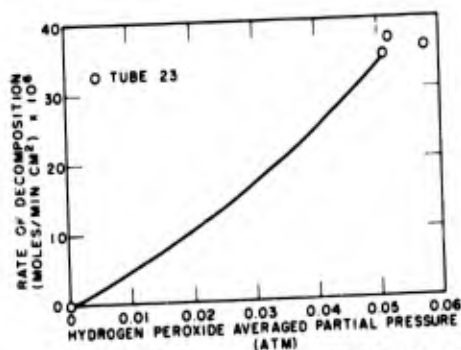


FIG 16 DECOMPOSITION RATE OF HYDROGEN PEROXIDE VAPOR ON A LEAD GLASS SURFACE TREATED WITH 4N PHOSPHORIC ACID (T = 215°C)

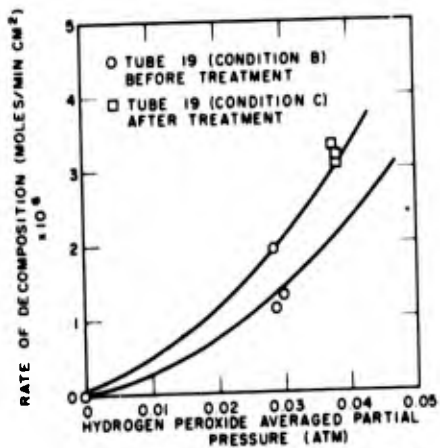


FIG 17 EFFECT OF TREATING A PYREX SURFACE WITH 200 PPM SODIUM STANNATE SOLUTION ON THE DECOMPOSITION RATE OF HYDROGEN PEROXIDE VAPOR (T=215°C)

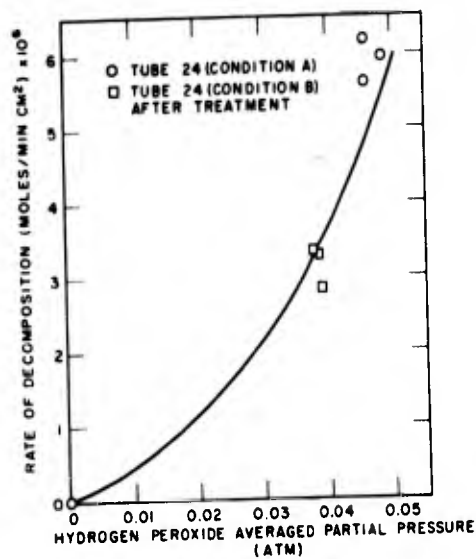


FIG 18 EFFECT OF PASSING GASEOUS SO<sub>2</sub> OVER PYREX SURFACE ON THE DECOMPOSITION RATE OF HYDROGEN PEROXIDE VAPOR (T = 215°C)

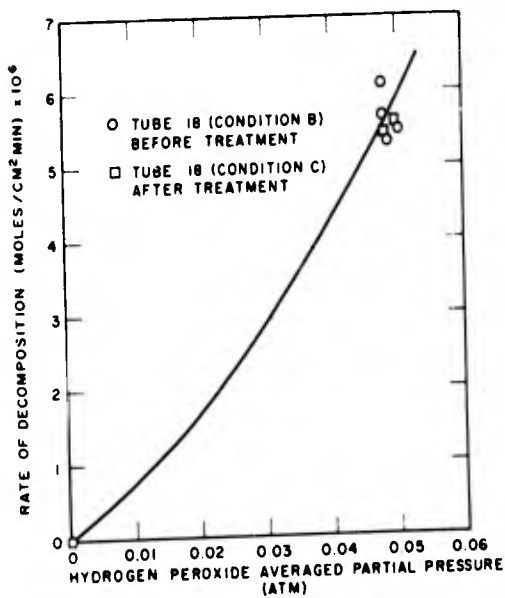


FIG 19 EFFECT OF TREATING A PYREX SURFACE WITH HYDROGEN PEROXIDE LIQUID ON THE DECOMPOSITION RATE OF HYDROGEN PEROXIDE VAPOR (T=215°C)

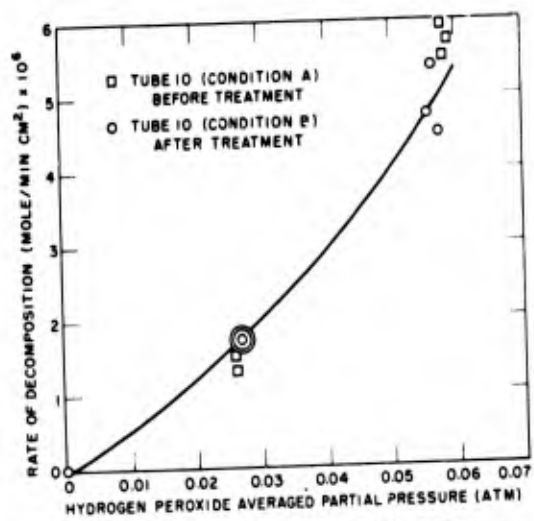


FIG 20 EFFECT OF TREATING A PYREX SURFACE WITH A METAKAOLIN SLIP ON THE DECOMPOSITION RATE OF HYDROGEN PEROXIDE VAPOR (T = 215°C)

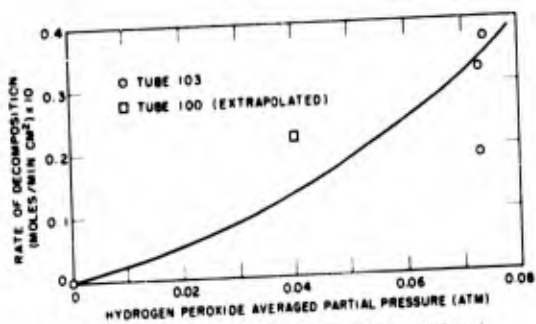


FIG 21 DECOMPOSITION RATE OF HYDROGEN PEROXIDE VAPOR ON A FUSED-ACID TREATED PYREX SURFACE (T = 215°C)

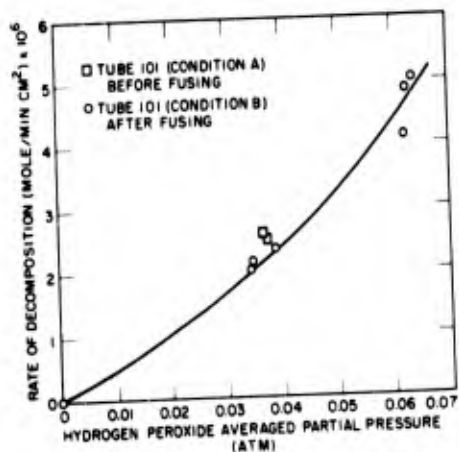


FIG 24 EFFECT OF FUSING A PYREX SURFACE WITH A FLAME ON THE DECOMPOSITION RATE OF HYDROGEN PEROXIDE VAPOR (T = 215°C)

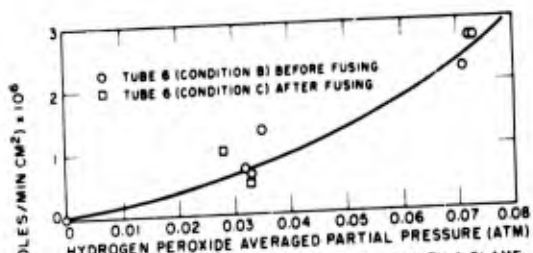


FIG 22 EFFECT OF FUSING A PYREX SURFACE WITH A FLAME ON THE DECOMPOSITION RATE OF HYDROGEN PEROXIDE VAPOR (T = 215°C)

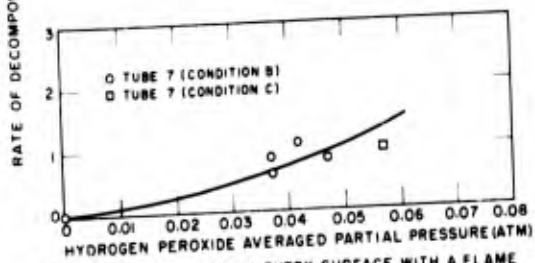


FIG 23 EFFECT OF FUSING A PYREX SURFACE WITH A FLAME ON THE DECOMPOSITION RATE OF HYDROGEN PEROXIDE VAPOR (T = 215°C)

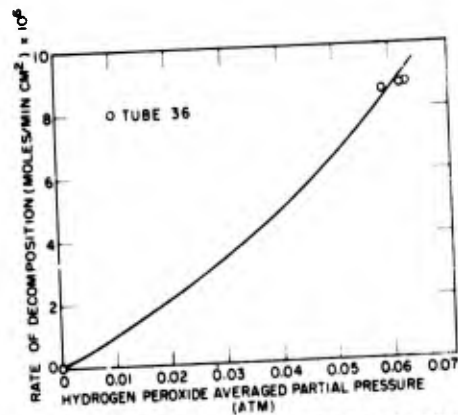


FIG 25 EFFECT OF FUSING A PYREX SURFACE AT 430°C ON THE DECOMPOSITION RATE OF HYDROGEN PEROXIDE VAPOR (T = 215°C)

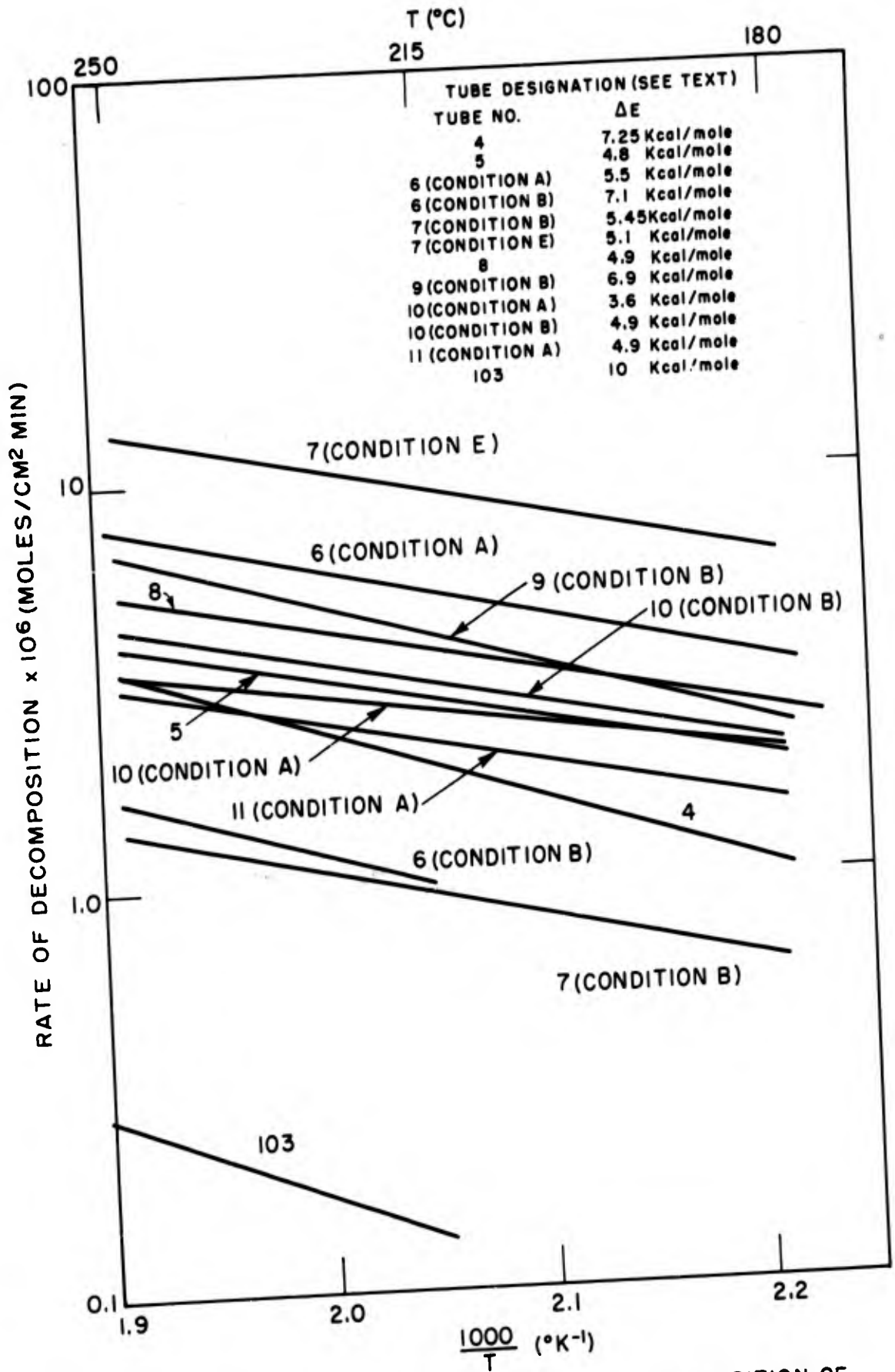


FIG. 26 EFFECT OF TEMPERATURE ON THE DECOMPOSITION OF HYDROGEN PEROXIDE VAPOR ( $P_{H_2O_2} = 0.04$  ATM)

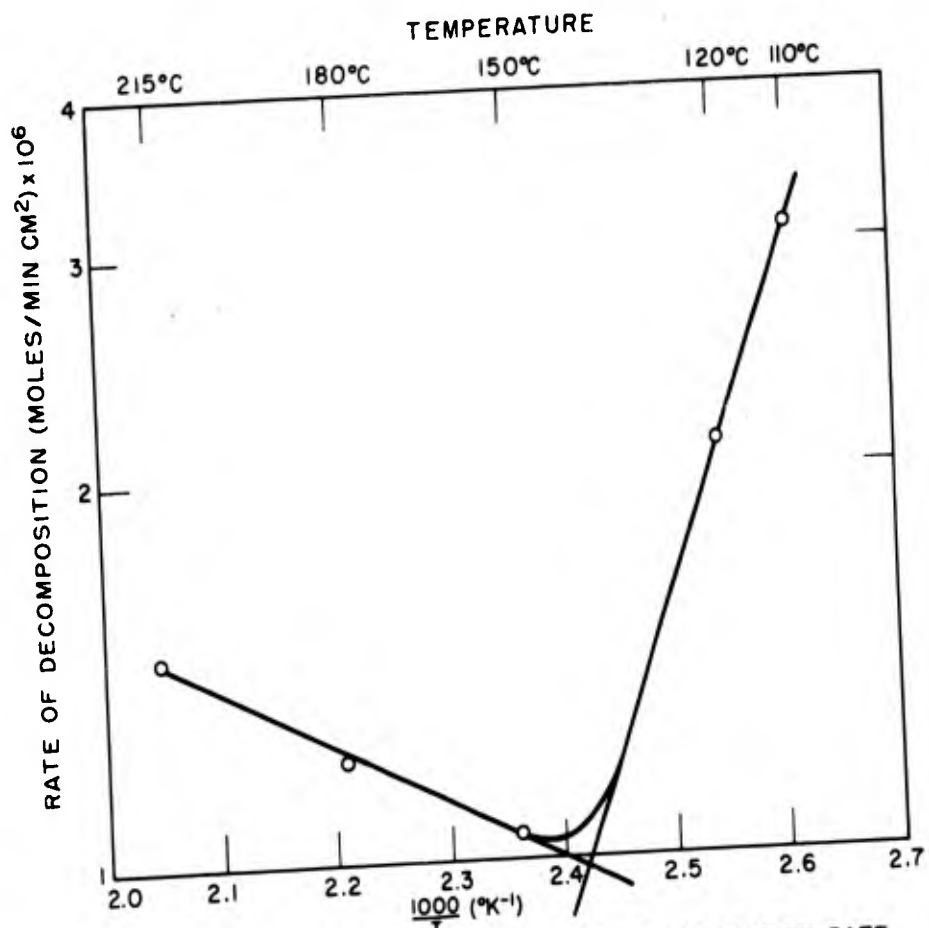


FIG. 27 EFFECT OF TEMPERATURE ON THE DECOMPOSITION RATE OF HYDROGEN PEROXIDE VAPOR ( $P_{H_2O_2} = 0.02$  ATM)

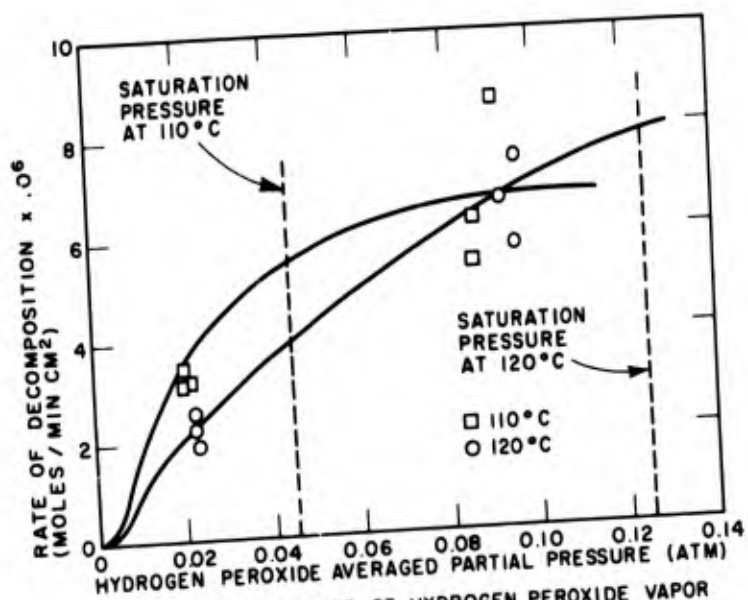


FIG. 28 DECOMPOSITION RATE OF HYDROGEN PEROXIDE VAPOR ON A PYREX SURFACE ( $T = 110^\circ\text{C}$  AND  $120^\circ\text{C}$ )

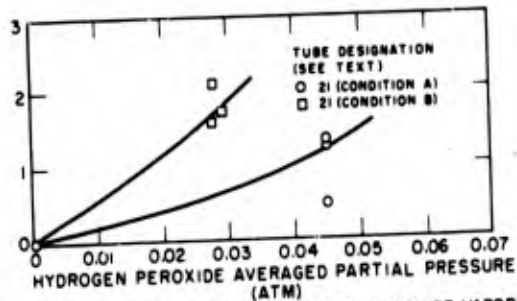


FIG. 29 DECOMPOSITION RATE OF HYDROGEN PEROXIDE VAPOR ON A PYREX SURFACE COATED WITH FLUOROLUBE GREASE ( $T = 215^{\circ}\text{C}$ )

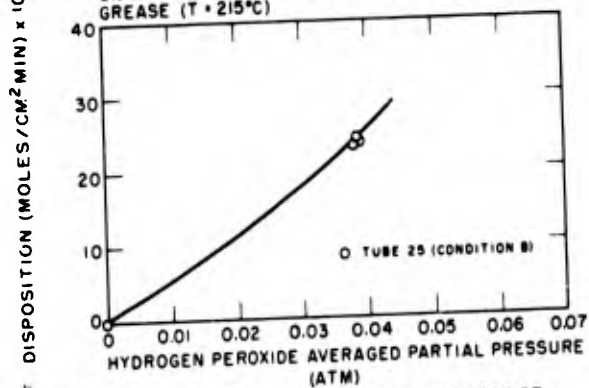


FIG. 30 DECOMPOSITION RATE OF HYDROGEN PEROXIDE VAPOR ON A TEFLON SURFACE ( $T = 215^{\circ}\text{C}$ )

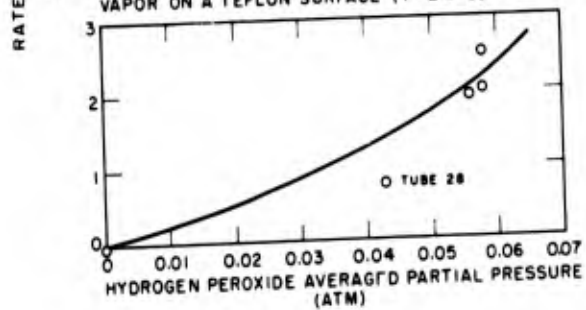


FIG. 31 DECOMPOSITION RATE OF HYDROGEN PEROXIDE VAPOR ON A PYREX SURFACE COATED WITH METHYL TRICHLORO SILANE ( $T = 215^{\circ}\text{C}$ )

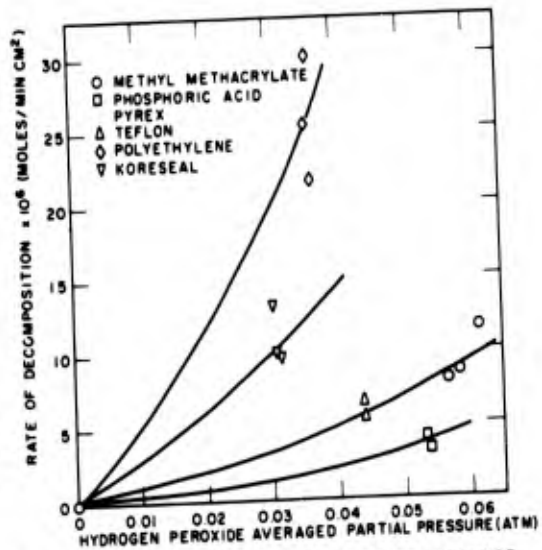


FIG. 32 DECOMPOSITION RATE OF HYDROGEN PEROXIDE VAPOR ON VARIOUS PLASTIC SURFACES ( $T = 120^{\circ}\text{C}$ )

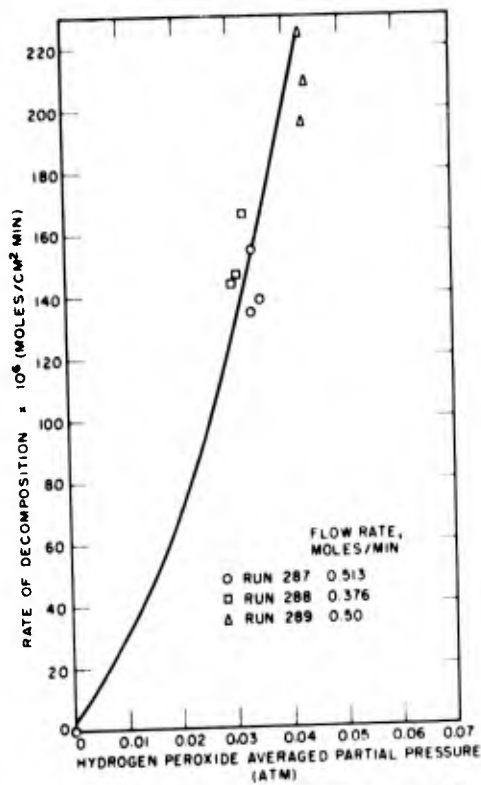


FIG 33- DECOMPOSITION RATE OF HYDROGEN PEROXIDE VAPOR ON AN ELECTROPOLISHED STAINLESS STEEL 304 SURFACE (T = 150°C)

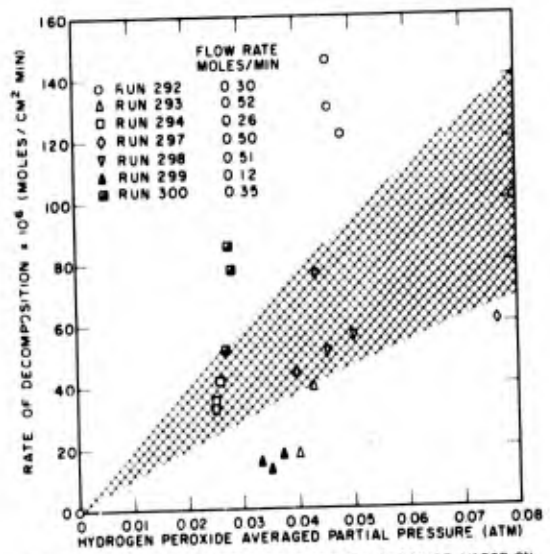


FIG 34 DECOMPOSITION RATE OF HYDROGEN PEROXIDE VAPOR ON AN ELECTROPOLISHED STAINLESS STEEL 304 SURFACE (T = 150°C)

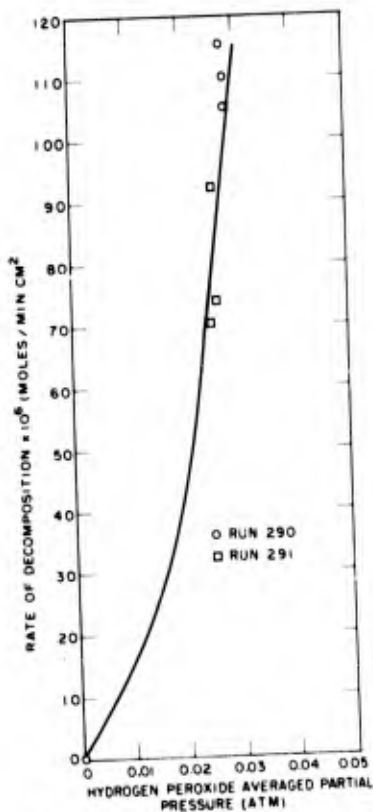


FIG 35 DECOMPOSITION RATE OF HYDROGEN PEROXIDE VAPOR ON AN ELECTRO-POLISHED STAINLESS STEEL 416 SURFACE (T = 150°C)

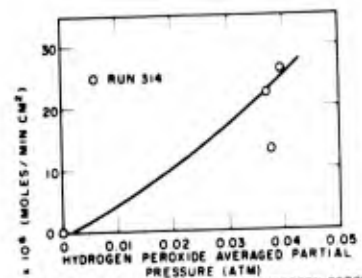


FIG 36 DECOMPOSITION RATE OF HYDROGEN PEROXIDE VAPOR ON A PASSIVATED STAINLESS STEEL 303 SURFACE (T = 150°C)

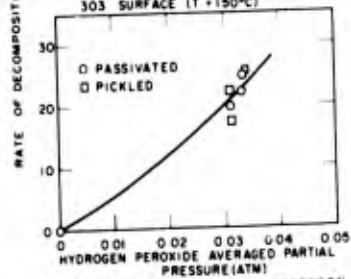


FIG 37 DECOMPOSITION RATE OF HYDROGEN PEROXIDE VAPOR ON PASSIVATED AND PICKLED STAINLESS STEEL 304 SURFACES (T = 150°C)

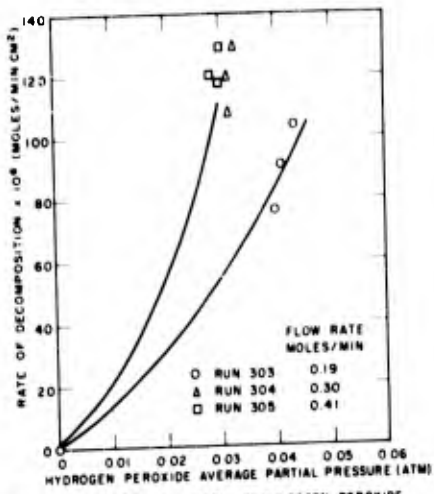


FIG 38 DECOMPOSITION RATE OF HYDROGEN PEROXIDE VAPOR ON ELECTROPOLISHED 25 ALUMINUM SURFACE (T=150°C)

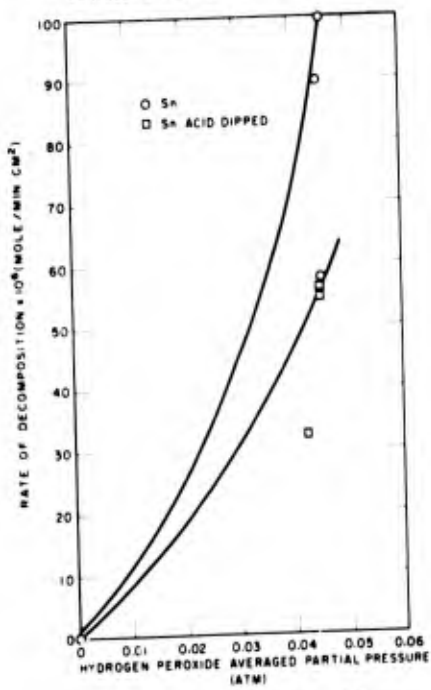


FIG 41 DECOMPOSITION RATES OF HYDROGEN PEROXIDE VAPOR ON TIN SURFACES (T=150°C)

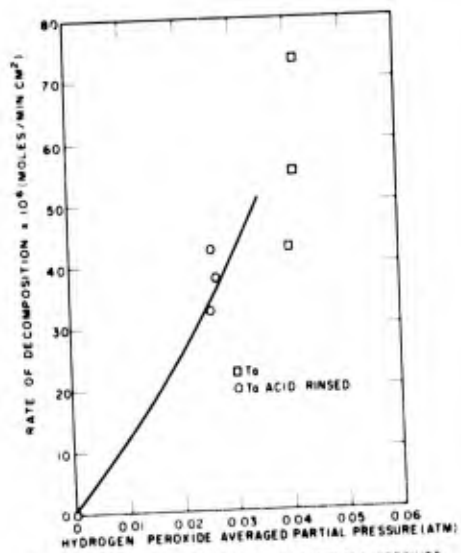


FIG 42 DECOMPOSITION RATES OF HYDROGEN PEROXIDE VAPOR ON TANTALUM SURFACES (T=150°C)

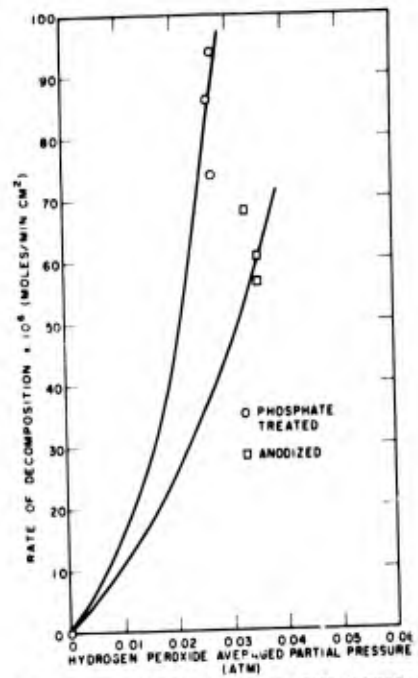


FIG 39 DECOMPOSITION RATE OF HYDROGEN PEROXIDE VAPOR ON PHOSPHATED AND ANODIZED 25 ALUMINUM SURFACES (T=150°C)

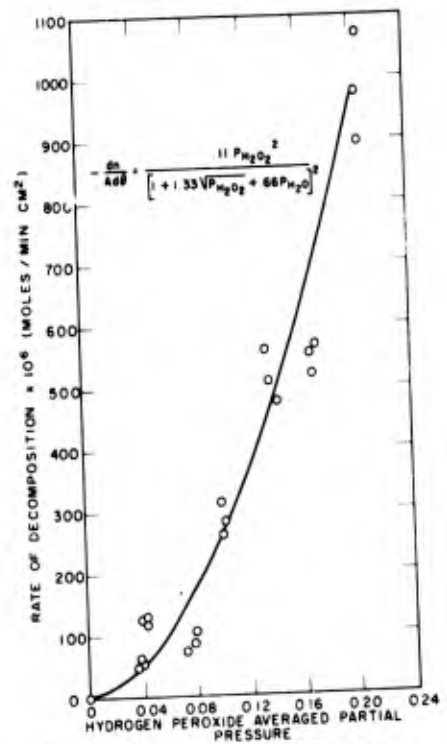


FIG 40 DECOMPOSITION RATE OF HYDROGEN PEROXIDE VAPOR ON A PICKLED 25 ALUMINUM SURFACE (T=150°C)

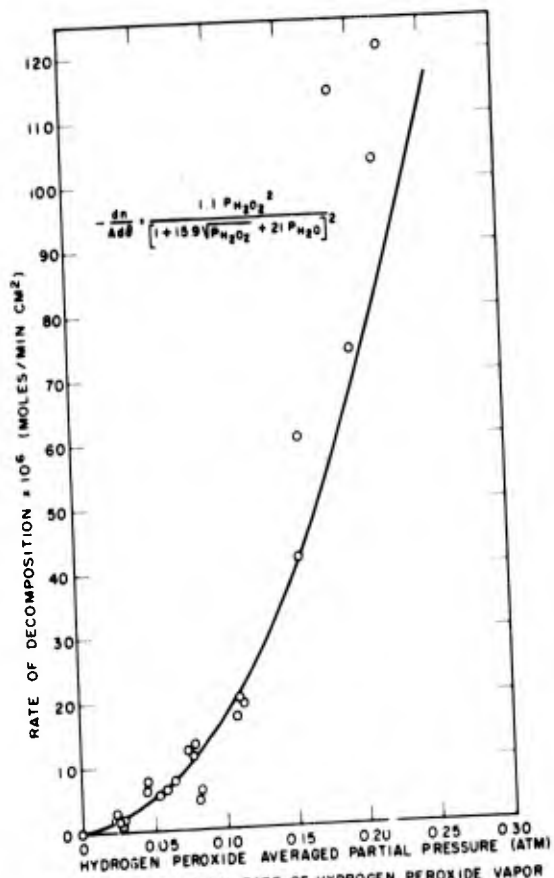


FIG 43 DECOMPOSITION RATE OF HYDROGEN PEROXIDE VAPOR ON BORIC OXIDE SURFACE (TUBE 9) (T=180°C)

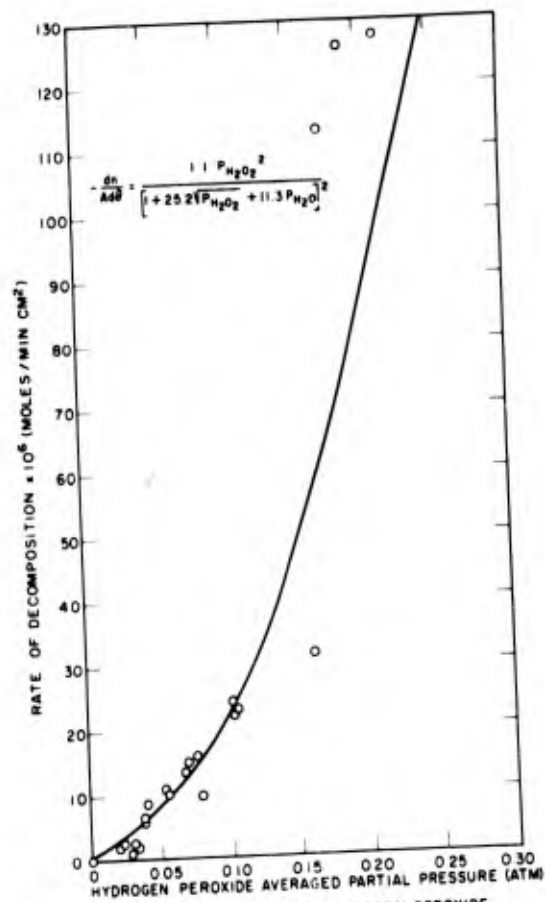


FIG 44 DECOMPOSITION RATE OF HYDROGEN PEROXIDE VAPOR ON BORIC OXIDE SURFACE (TUBE 9) (T=215°C)

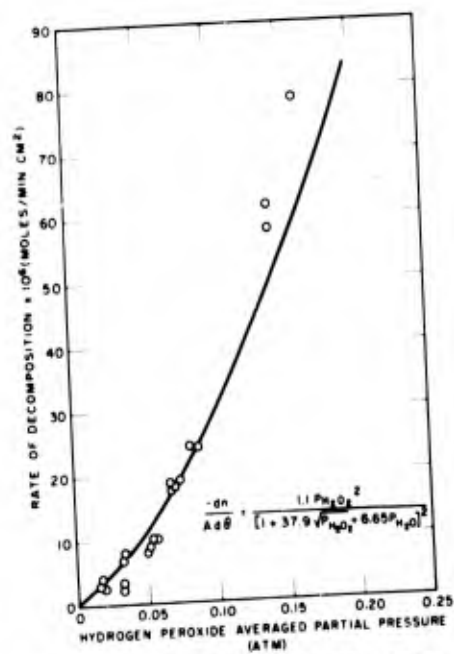


FIG 45 DECOMPOSITION RATE OF HYDROGEN PEROXIDE VAPOR ON BORIC OXIDE SURFACE (TUBE 9) (T=250°C)

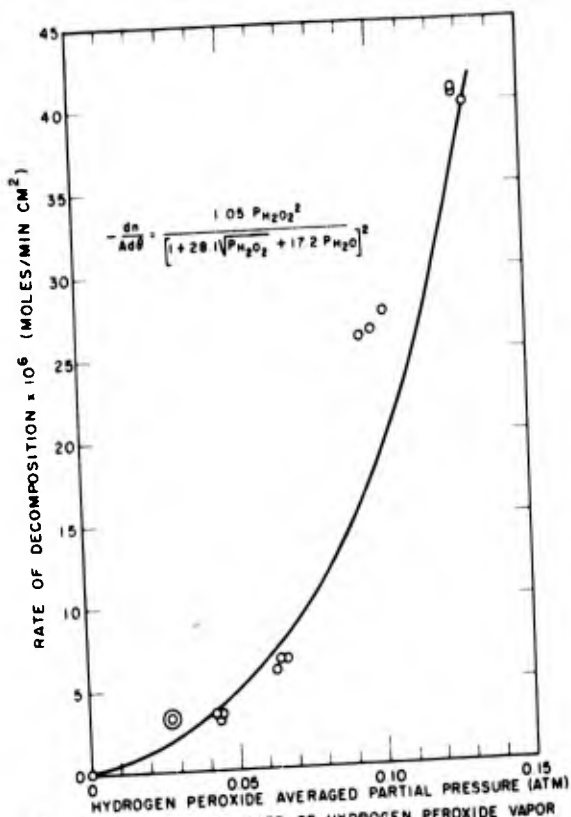


FIG 46 DECOMPOSITION RATE OF HYDROGEN PEROXIDE VAPOR ON BORIC OXIDE SURFACE (TUBE 9 PLUS RODS) (T = 180°C)

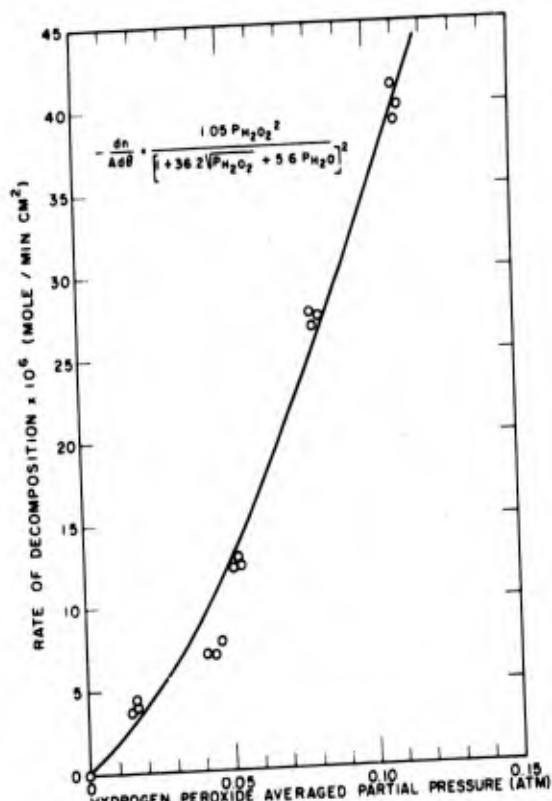


FIG 47 DECOMPOSITION RATE OF HYDROGEN PEROXIDE VAPOR ON BORIC OXIDE SURFACES (TUBE 9 PLUS RODS) (T = 215°C)

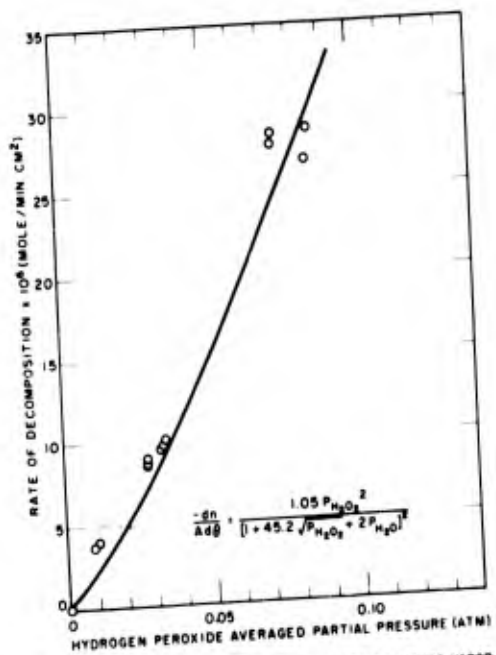


FIG 48 DECOMPOSITION RATE OF HYDROGEN PEROXIDE VAPOR ON BORIC OXIDE SURFACE (TUBE 9 PLUS RODS) (T = 250°C)

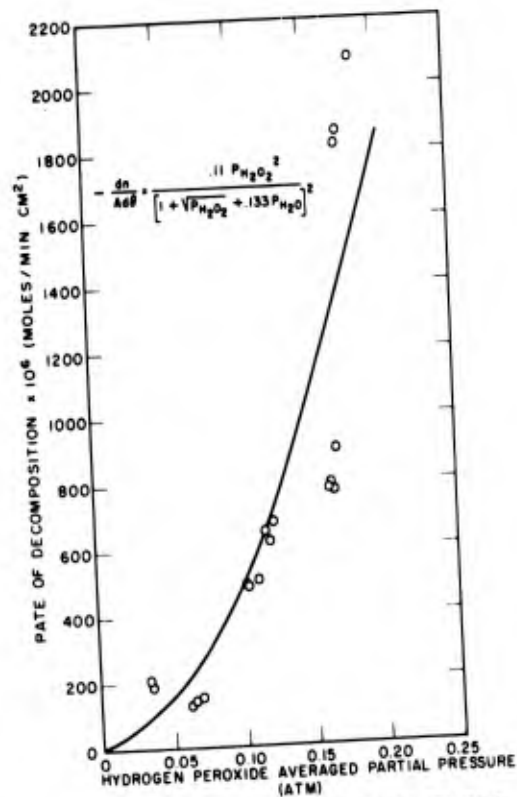


FIG 49 DECOMPOSITION RATE OF HYDROGEN PEROXIDE VAPOR ON PICKLED 25 ALUMINUM SURFACE (T = 180°C)

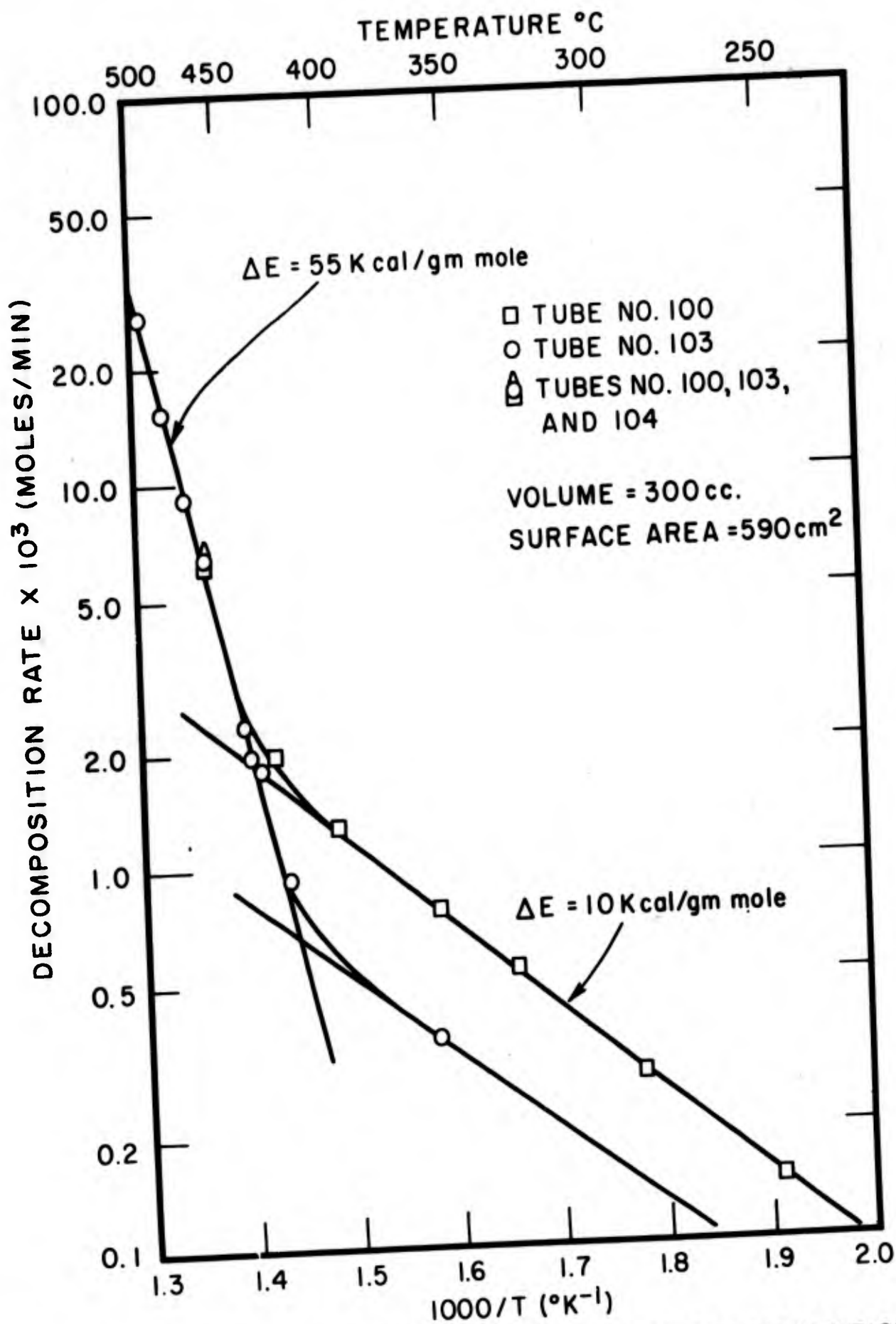


FIG. 50 - EFFECT OF TEMPERATURE ON THE DECOMPOSITION OF HYDROGEN PEROXIDE VAPOR. ( $p_{H_2O_2} = 0.02$  ATM.)

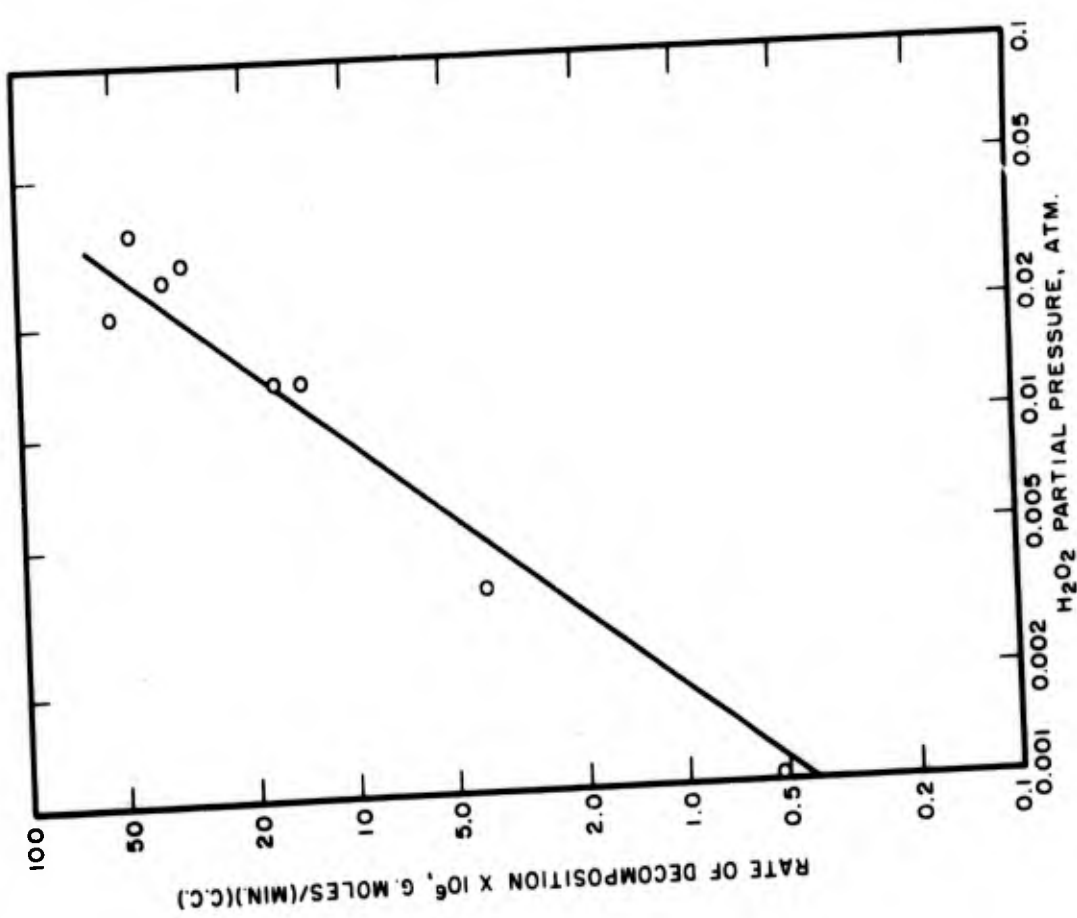


FIG. 52 - EFFECT OF CONCENTRATION ON THE HOMOGENEOUS DECOMPOSITION RATE OF H<sub>2</sub>O<sub>2</sub> (FROM HUANG), T = 475°C

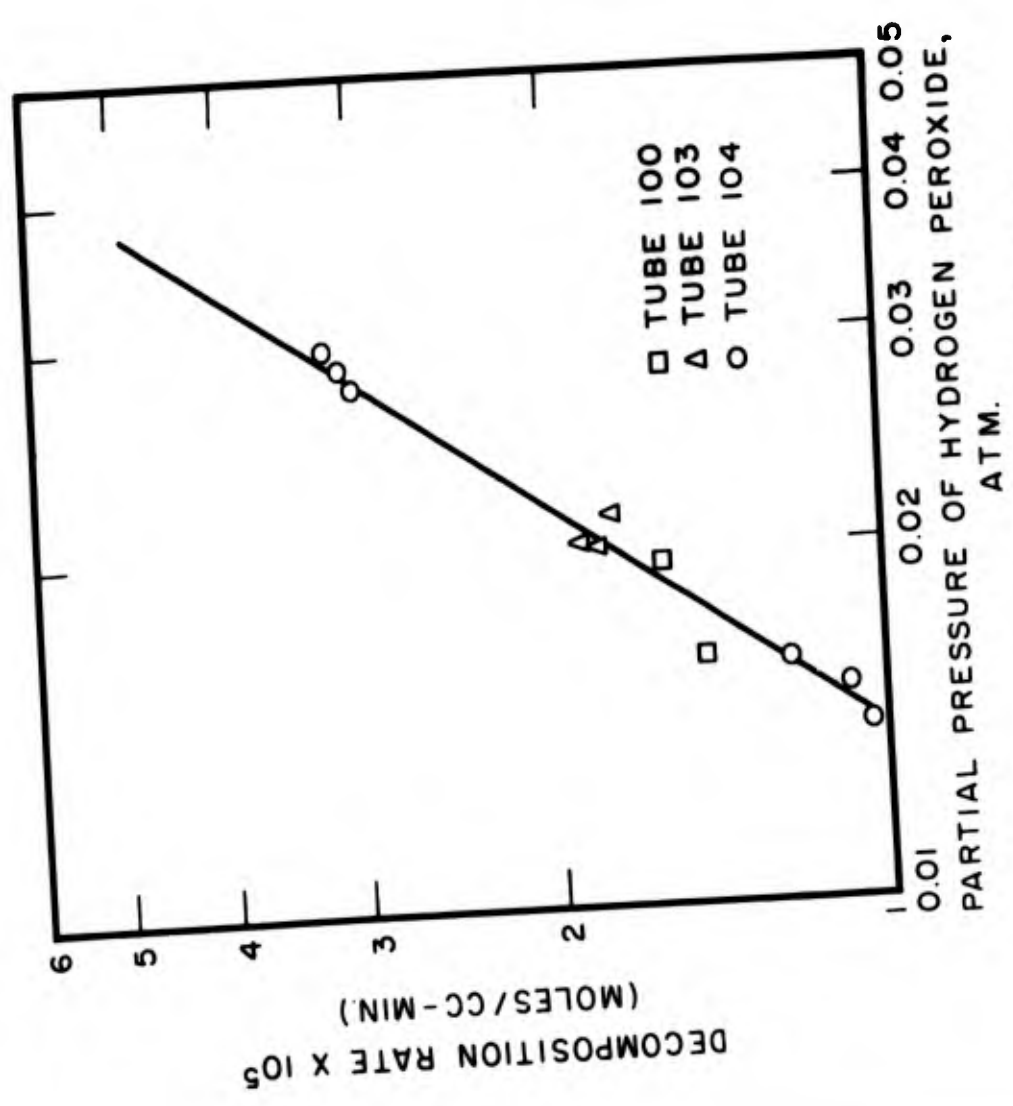


FIG. 51 - EFFECT OF CONCENTRATION ON THE HOMOGENEOUS DECOMPOSITION RATE OF HYDROGEN PEROXIDE. T = 460°C



FIG. A1 - TWO DIMENSIONAL REPRESENTATION OF BORIC OXIDE GLASS

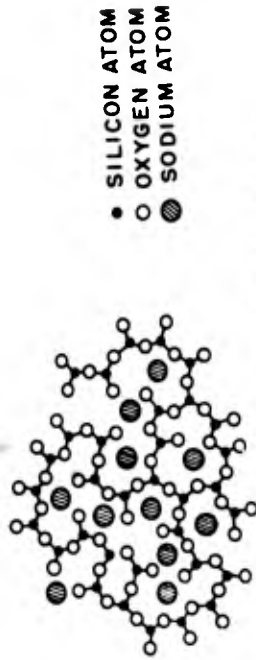


FIG. A2 - SCHEMATIC REPRESENTATION IN TWO DIMENSIONS OF THE STRUCTURE OF SODA-SILICA GLASS

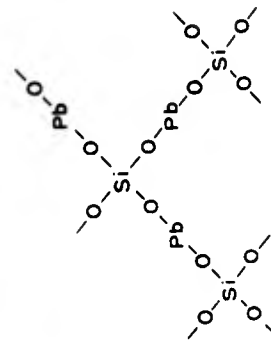


FIG. A3 - REPRESENTATION OF LEAD GLASS

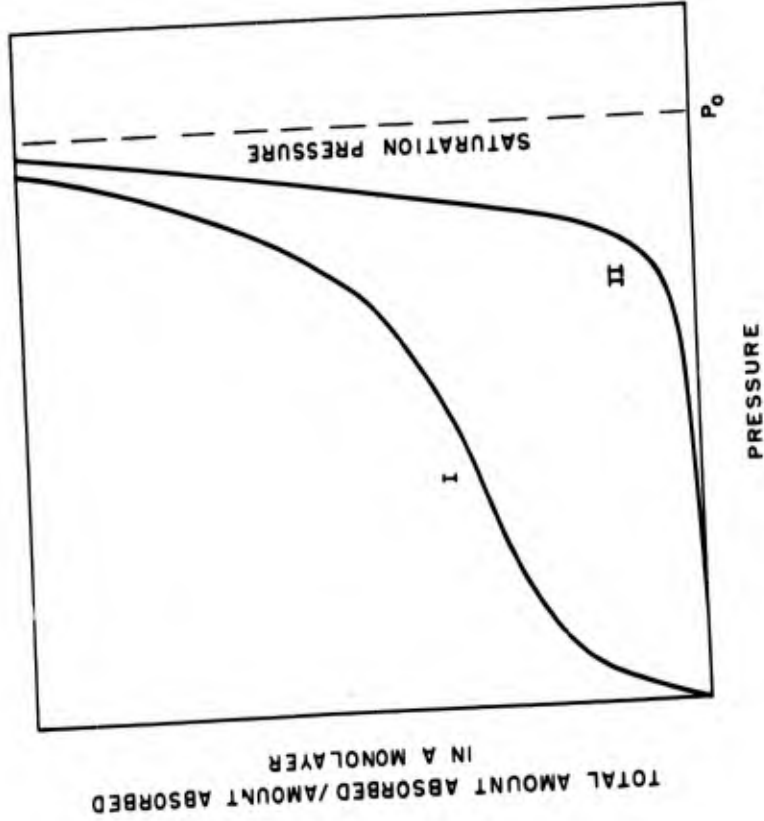


FIG. A4 MULTILAYER ABSORPTION ISOTHERM

**DISTRIBUTION LIST  
CONTRACT N5ori 07819  
STABILITY AND REACTION STUDIES  
OF HYDROGEN PEROXIDE**

**MASSACHUSETTS INSTITUTE OF TECHNOLOGY  
CAMBRIDGE, MASSACHUSETTS**

<u>Addressee</u>	<u>Transmitted Via</u>	<u>Number of Copies</u>	<u>Addressee</u>	<u>Transmitted Via</u>	<u>Number of Copies</u>
Committee on Guided Missiles Office of the Secretary of Defense (RAD) Room 3D-125, The Pentagon Washington 25, D. C.		1	Chief, Research and Engineering Division Office, Chief of Chemical Corps. Army Chemical Center, Maryland		1
Chief of Staff, U. S. Air Force The Pentagon Washington 25, D. C. Attn: DCS/D, AFDRD-AC-2 DCS/D, AFOP-00		1	Commanding Officer USS Norton Sound (AVM-1) c/o Fleet Post Office San Francisco, California		1
Commanding General Air Materiel Command Wright-Patterson Air Force Base Dayton, Ohio Attn: MCREXP WCLPR-4		2	Commanding General White Sands Proving Ground Las Cruces, New Mexico		1
Chief, Bureau of Aeronautics Department of the Navy Washington 25, D. C. Attn: T-4 SI-592		1	Technical Library Atomic Energy Commission 1901 Constitution Avenue Washington 25, D. C. Attn: Mr. F. E. Fry		1
Chief, Bureau of Ordnance Department of the Navy Washington 25, D. C. Attn: H66A H69 H62D		3	Commandant of the Marine Corps Headquarters, U. S. Marine Corps. Washington 25, D. C. Attn: S-4 (Ordnance)		1
Chief, Bureau of Ships Department of the Navy Washington 25, D. C. Attn: Code 541 Code 430 Code 530 Code 533 Code 519		1	Commander Operational Development Force U. S. Naval Base Norfolk 14, Virginia		1
U. S. Naval Air Rocket Test Station Lake Denmark Dover, New Jersey Attn: Dr. T. Shineradit		1	Office, Asst. Chief of Staff (3-4) Research & Development Division Department of the Army The Pentagon Washington 25, D. C.		1
Commander Naval Air Materiel Center Philadelphia 12, Pennsylvania		1	Head of Ordnance and Gunnery U. S. Naval Academy Annapolis, Maryland		1
Commander U. S. Naval Air Missile Test Center Point Mugu, California		1	Commanding Officer U. S. Naval Underwater Ordnance Station New Port, Bermuda Island		2
Commander U. S. Naval Ordnance Test Station Inyokern, California P. O. China Lake, California Attn: Reports Unit Code 4012		1	Naval Inspector of Ordnance Electric Boat Company Groton, Connecticut		1
Director National Advisory Committee for Aeronautics 1724 F Street, NW Washington 25, D. C. Attn: Mr. C. H. Helms		2	Director U. S. Naval Engineering Experiment Station Annapolis, Maryland		1
Director U. S. Naval Research Laboratory Office of Naval Research, Annapolis Washington 25, D. C. Attn: Code 3280 Code 2000		1 6 (if class if. only 1)	Director Office of Naval Research Branch Office 150 Caseway Street Boston 10, Massachusetts		2
Chief of Naval Research Department of the Navy Washington 25, D. C. Attn: Code 429		3 (if classif. 13)	Director Office of Naval Research Branch Office 134 Broadway New York 13, New York		1
Commanding Officer Frankford Arsenal Philadelphia 37, Pennsylvania Attn: Fire Control Division		1	Director Office of Naval Research Branch Office 1000 Jeary Street San Francisco 9, California		1
Superintendent U. S. Naval Postgraduate School Monterey, California Attn: Librarian		1	Director Office of Naval Research Branch Office 1030 Green Street Pasadena 1, California		1
Department of the Army Office, Chief of Ordnance The Pentagon Washington 25, D. C. Attn: CRDTU		1	Director Office of Naval Research Branch Office Tenth Floor The John Crerar Library Building 86 East Randolph Street Chicago 1, Illinois		1
Commander Naval Ordnance Laboratory, White Oak Silver Spring 19, Maryland Attn: The Library, Room 10333		1	Officer-in-Charge Office of Naval Research Navy No. 100 Fleet Post Office New York, New York		2
Commanding General AAA and 3M Center Fort Bliss, Texas		1	Commanding General Air Research & Development Command P. O. Box 1395 Baltimore 3, Maryland Attn: RDRRC		1
Chief of Naval Operations Department of the Navy Washington 25, D. C. Attn: Op-51		1	Dr. Martin Kilpatrick Department of Chemistry Illinois Institute of Technology 1300 Federal Street Chicago 16, Illinois	If Classified Via: Director Office of Naval Research Branch Office Tenth Floor The John Crerar Library Building 86 E. Randolph St. Chicago 1, Ill.	1
			State Engineering Experimental Station Georgia Institute of Technology Atlanta, Georgia	Bureau of Ships (Code 620) Department of the Navy Washington 25, D. C.	1

Address	Transmitted Via (If Classified Via)	Number of Copies	Address	Transmitted Via (If Classified Via)	Number of Copies
Applied Physics Laboratory Johns Hopkins University Silver Spring, Maryland Attn: Dr. Dwight E. Gray	Naval Inspector of Ordnance Applied Physics Lab. Johns Hopkins University 8621 Georgia Avenue Silver Spring, Maryland	1	Electrochemical Department Technical Division E. I. duPont de Nemours & Co. Inc. Niagara Falls, New York Attn: Dr. D. Campbell	Inspector of Naval Material Room 505-508 Post Office Building Buffalo 3, New York	1
Bell Aircraft Corporation Niagara Falls, New York Attn: Mr. R. B. Foster	U. S. Air Force Plant Representative Niagara Falls, New York	1	Buffalo Electro-Chemical Co. Buffalo 7, New York Attn: Dr. N. S. Davis	Inspector of Naval Material Room 505-508 Post Office Building Buffalo 3, New York	1
Consolidated-Vultee Aircraft Corp. San Diego 12, Calif. Attn: Mr. J. V. Naish	Bureau of Aeronautics Representative Consolidated-Vultee Aircraft Corp. San Diego 12, Calif.	1	Walter Kilde and Co., Inc. Belleville, New Jersey Attn: Project MX-922 Contract AF(33-036)3897	Inspector of Naval Material Naval Industrial Reserve Shipyard Bldg. 13, Port Newark Newark 3, New Jersey	1
Douglas Aircraft 3000 Ocean Blvd. Santa Monica, Calif. Attn: Mr. E. F. Burton	District Chief Los Angeles Ordnance District 35 No. Raymond Ave. Pasadena 1, Calif.	1	Redal Incorporated 401 East Juliana Street Anaheim, California	Inspector of Naval Material 1206 South Street Los Angeles 15, California	1
Rand Corporation 1500 Fourth Street Santa Monica, Calif. Attn: Mr. F. R. Colibohn	Chief, Los Angeles AFPO 155 West Washington Blvd. Los Angeles 54, Calif.	1	Armed Services Technical Information Agency Documents Service Center Knott Building Dayton 2, Ohio	5 (Uncl. only)	
General Electric Company Project HERMES Schenectady, New York Attn: Mr. C. K. Bauer	Resident Ordnance Officer Project HERMES Campbell Avenue Plant General Electric Company Schenectady 5, New York	1	Office of Technical Services Department of Commerce Washington 25, D. C.	1 (Uncl. only)	
Glenn L. Martin Company Baltimore 3, Maryland Attn: Mrs. Lucille Walper	Bureau of Aeronautics Representative Glenn L. Martin Company Baltimore 3, Maryland	1	Thompson Products, Inc. Staff Research and Development 2196 Clarkwood Cleveland 3, Ohio Attn: A. G. Kresse	Bureau of Aeronautics Thompson Products, Inc. Cleveland 3, Ohio	1
California Institute of Technology Jet Propulsion Laboratory Pasadena, California	District Chief Los Angeles Ordnance District 35 North Raymond Avenue Pasadena 1, California	1	Communications General Bedstone Arsenal Huntsville, Alabama Attn: Technical Library	1	
North American Aviation, Inc. 12214 Lakewood Blvd. Downey, California Attn: Group 95-17	Air Force Plant Rep. WEAPT North American Aviation Inc. Los Angeles International Airport Los Angeles 48, California	1	Hayden Library M.I.T. Room 148-226 Attention: Miss Bartlett Special Collections Librarian	2 (Uncl. only)	
Princeton University Princeton, New Jersey Attn: Project SQUID	Commanding Officer Office of Naval Research Branch Office 346 Broadway New York 17, New York	1			
University of Michigan Aeronautical Research Center Willow Run Airport Ypsilanti, Michigan Attn: Mr. L. R. Blase, 1	Commanding Officer Central Air Procurement Division West Warren & Lonyo Avenues Detroit 32, Michigan	1			
Aerojet-General Corporation Azusa, California Attn: Dr. D. L. Armstrong	Bureau of Aeronautics Representative Aerojet-General Corp. Azusa, California	1			
Battelle Memorial Institute 505 King Avenue Columbus 1, Ohio Attn: Dr. B. D. Thomas	Air Regional Representative Dayton Regional Office Central Air Procurement Acol. U. S. Bldg., Dayton 1, Ohio	1			
Bethlehem Steel Corporation Shipbuilding Division Quincy 60, Massachusetts Attn: Mr. B. Fox	Supervisor of Shipbuilding, USN Bethlehem Steel Corp. Quincy 69, Massachusetts	1			
Experiment Incorporated Richmond, Virginia Attn: Dr. J. W. Kullen, 11	Naval Inspector of Ordnance Applied Physics Laboratory Johns Hopkins University 8621 Georgia Avenue Silver Spring, Maryland	1			
Detroit Controls Company Research Division Redwood City, California	Asst. Inspector of Naval Material 533 Middlefield Rd. Redwood City, California	1			
Fairchild Engine and Airplane Corp. Fairchild Engine Division Farmingdale, Long Island, New York Attn: Mr. E. M. Lester	Bureau of Aeronautics Rep. Fairchild Engine & Airplane Corp. Farmingdale, Long Island, New York	1			
Purdue University Lafayette, Indiana Attn: Dr. M. J. Zucrow	Office of Naval Research branch Office The John Crerar Library Bldg. 10th Floor, 86 E. Randolph Street Chicago 1, Illinois	1			
Reaction Motors, Inc. Stickle Avenue & Elm Street Rookaway, New Jersey	Bureau of Aeronautics Rep. Reaction Motors, Inc. Stickle Avenue & Elm St. Rookaway, New Jersey	1			
United States Rubber Company General Laboratories Passaic, New Jersey Attn: Mr. C. E. Hurdia	Inspector of Naval Material Naval Industrial Reserve Shipyard Bldg. 13, Port Newark Newark 3, New Jersey	1			

**AD**

**83341**

**Armed Services Technical Information Agency**

**Reproduced by  
DOCUMENT SERVICE CENTER  
KNOTT BUILDING, DAYTON, 2, OHIO**

This document is the property of the United States Government. It is furnished for the duration of the contract and shall be returned when no longer required, or upon recall by ASTIA to the following address:  
Armed Services Technical Information Agency, Document Service Center,  
Knott Building, Dayton 2, Ohio.

**NOTICE: WHEN GOVERNMENT OR OTHER DRAWINGS, SPECIFICATIONS OR OTHER DATA ARE USED FOR ANY PURPOSE OTHER THAN IN CONNECTION WITH A DEFINITELY RELATED GOVERNMENT PROCUREMENT OPERATION, THE U. S. GOVERNMENT THEREBY INCURS NO RESPONSIBILITY, NOR ANY OBLIGATION WHATSOEVER; AND THE FACT THAT THE GOVERNMENT MAY HAVE FORMULATED, FURNISHED, OR IN ANY WAY SUPPLIED THE SAID DRAWINGS, SPECIFICATIONS, OR OTHER DATA IS NOT TO BE REGARDED BY IMPLICATION OR OTHERWISE AS IN ANY MANNER LICENSING THE HOLDER OR ANY OTHER PERSON OR CORPORATION, OR CONVEYING ANY RIGHTS OR PERMISSION TO MANUFACTURE, USE OR SELL ANY PATENTED INVENTION THAT MAY IN ANY WAY BE RELATED THERETO.**

**UNCLASSIFIED**